Classification: Original article

Hepatocyte growth factor-induced c-Src-phosphatidylinositol 3-kinase-AKT-mammalian target of rapamycin pathway inhibits dendritic cell activation by blocking IκB kinase activity

Eshu Singhal and Pradip Sen

Division of Cell Biology and Immunology, Institute of Microbial Technology, Council of Scientific and Industrial Research, Chandigarh, India.

Correspondence should be addressed to:

Pradip Sen, Ph.D
Division of Cell Biology and Immunology
Institute of Microbial Technology
Sector-39A, Chandigarh-160036, India.
Email Address: psen@imtech.res.in
Tel#: + 091-172-2636680 Extn-280
Fax#: + 091-172-2690585

ABSTRACT

Hepatocyte growth factor modulates activation and antigen-presenting cell function of dendritic cells. However, the molecular basis for immunoregulation of dendritic cells by hepatocyte growth factor is undefined. In the current study, we demonstrate that hepatocyte growth factor exhibits inhibitory effect on dendritic cell activation by blocking IκB kinase activity and subsequent nuclear factor-κB activation. Inhibition of IκB kinase is mediated by hepatocyte growth factor-induced activation of c-Src. Proximal signaling events induced in dendritic cells by hepatocyte growth factor include a physical association of c-Src with the hepatocyte growth factor receptor c-MET and concomitant activation of c-Src. Activation of c-Src in turn establishes a complex consisting of phosphatidylinositol 3-kinase and c-MET, and promotes downstream activation of the phosphatidylinositol 3-kinase/AKT pathway and mammalian target of rapamycin. Blocking activation of c-Src, phosphatidylinositol 3-kinase and mammalian target of rapamycin prevents hepatocyte growth factor-induced inhibition of IκB kinase, nuclear factor-κB and dendritic cell activation. Notably, hepatocyte growth factor-stimulated c-Src activation results in induction of phosphatidylinositol 3-kinase complexes p85α/p110α and p85α/p110δ; which is required for activation of mammalian target of rapamycin, and consequent inhibition of IκB kinase and nuclear factor-κB activation. Our findings, for the first time, have identified the c-Src-phosphatidylinositol 3-kinase-AKT-mammalian target of rapamycin pathway that plays a pivotal role in mediating the inhibitory effects of hepatocyte growth factor on dendritic cell activation by blocking nuclear factor-κB signaling.

Keywords: c-MET / dendritic cell / hepatocyte growth factor / NF-κB / signaling

1. INTRODUCTION

Among antigen-presenting cells (APCs), only dendritic cells (DCs) are capable of activating naïve T cells to initiate a primary immune response (Hilkens et al., 1997). However, the outcome of a T cell response is largely dependent on the activation and maturation status of DCs. Immature DCs, which express low levels of major histocompatibility complex (MHC) and costimulatory molecules, exhibit a reduced T cell stimulatory capacity (Jonuleit et al., 2000). Upon maturation, DCs upregulate expression of MHC and costimulatory molecules, and gain competency to promote expansion and effector T cell differentiation (Jonuleit et al., 2000). The maturation status of DCs is generally influenced by local cytokine milieu. Importantly, hepatocyte growth factor (HGF), which is a pleiotropic cytokine and expressed in immunosuppressive conditions such as tumors, is known to promote differentiation of monocytes to tolerogenic DCs (Rutella et al., 2006a, Rutella et al., 2006b). HGF treatment also results in suppression of DC function (Okunishi et al., 2005). Furthermore, a recent study demonstrates a role for HGF in induction of DC tolerance (Benkhoucha et al.). However, the molecular mechanism of HGF-induced inhibition of DC function has not been defined.

Although HGF was originally discovered as a potent mitogen for hepatocytes (Nakamura et al., 1984), it exhibits multiple effects on many other cell types. For example, HGF promotes mitogenesis, motogenesis and morphogenesis of a wide variety of cells; stimulates antigen-specific B cell differentiation, and migration of DCs and T cells; enhances neuron survival; and regulates leukocyte homing and lymph node organization (van der Voort et al., 1997, Zarnegar and Michalopoulos, 1995, Kurz et al., 2002,

Beilmann et al., 2000). Various studies further indicate that HGF exhibits immunoregulatory properties. For example, HGF is shown to counteract a potent immunosuppressive cytokine transforming growth factor β (TGFβ) (Ueki et al., 1999), which suggests that HGF might be an immunopotentiator. In contrast, the immunosuppressive effect of HGF is indicated by a report demonstrating that HGF prevents acute and chronic rejection of cardiac allograft by inducing TGFβ1 and IL-10 expression (Yamaura et al., 2004). HGF can mediate these different cellular functions because of its ability to activate multiple cytoplasmic signaling mediators. In fact, HGF triggers recruitment of a number of SH2-containing signal transducers such as phosphatidylinositol (PI) 3-kinase, Grb2-SOS complex, phospholipase C (PLC)-γ and c-Src to a multifunctional docking site YVHVNATYVNV located within HGF receptor cMET (Ponzetto et al., 1993, Ponzetto et al., 1994). Accordingly, it is important to define which signaling proteins are essential for inhibition of DCs by HGF.

Expression of several genes critical for activation, maturation and APC function of DCs is primarily regulated by a transcription factor nuclear factor-kappa B (NF-κB) (Rescigno et al., 1998, Weaver et al., 2001). NF-κB is a dimer composed of the Rel family of proteins and is sequestered in the cytoplasm of resting cells by inhibitory IκB proteins (Ghosh and Karin, 2002). Many external stimuli induce phosphorylation of IκBs by IκB kinase (IKK) complex, followed by proteolytic degradation of IκB proteins (Ghosh and Karin, 2002). However, role of the NF-κB pathway in HGF mediated immunoregulation of DCs remains unknown.

The signaling pathway transduced by c-MET in DCs upon HGF treatment is not yet defined. Therefore, the current study was initiated to determine the mechanism by which HGF regulates DC activation. We demonstrate that HGF-induced DC suppression requires activation of c-Src, which blocks the NF-κB pathway and subsequent DC activation via a signaling cascade involving sequential activation of the PI3K/AKT pathway and mammalian target of rapamycin (mTOR).

2. MATERIALS AND METHODS

2.1. Mice

BALB/c and C57/BL6 (B6) mice were maintained and bred under specific pathogen-free conditions. Use of mice was approved by the Institutional Animal Ethics Committee of the Institute of Microbial Technology, India.

2.2. DC preparation

Bone marrow-derived DCs (BMDCs) and splenic DCs (sDCs) were prepared from male or female BALB/c and B6 mice between 8-12 weeks of age as described (Bhattacharyya et al., 2004, Weaver et al., 2001). Flow cytometric analyses indicated ~90% purity of BMDCs and sDCs based on CD11c expression.

2.3. DC pretreatment with HGF, αc-MET Ab or inhibitors of signaling molecules

DCs ($5x10^6$ cells/well) were pretreated with specified concentrations of recombinant human HGF (Sigma-Aldrich, USA) for indicated times in 6-well low-cluster plates (Corning, USA) in RPMI 1640 complete medium (10% FBS, penicillin/streptomycin, L-glutamine, sodium pyruvate, non-essential amino acids, 2-mercaptoethanol). Subsequently, DCs were washed twice, resuspended in complete medium, and stimulated with lipopolysaccharide (LPS) (500 ng/ml) (Sigma-Aldrich, USA) or tumor necrosis factor α (TNFα) (20 ng/ml) (R&D Systems, USA) for specified times. In some experiments, DCs were treated for 1 h with (1) c-Src inhibitor E804 (10 nM; Calbiochem, USA), (2) PI3K inhibitors wortmannin (Wort) (200 nM; Cell Signaling Technology, USA) or Ly294002 (LY) (50 μM; Cell Signaling Technology, USA), (3) mTOR inhibitor

rapamycin (100 nM; Calbiochem, USA), or (4) 10 μg/ml αc-MET antibody (Ab) or isotype control Ab (R&D Systems, USA); or for 3 h with AKT inhibitor IV (AI-IV; 20 μM; Calbiochem, USA) before HGF treatment.

2.4. Electrophoretic mobility shift assay (EMSA) and Immunoblotting

Nuclear and cytoplasmic extracts were prepared from DCs as described (Beg et al., 1993). EMSA was performed using ^{32}P-labeled DNA probe containing NF-κB binding sites derived from MHC-I H2K promoter: 5'-CAGGGCTGGGGATTCCCCATCTCCACAGTTTCACTTC-3'(Haldar et al., 2010). A double stranded OCT-1 DNA probe, 5'-TGTCGAATGCAAATCACTAGAA-3' was used as control (Haldar et al., 2010). Supershift EMSAs were carried out as described (Haldar et al., 2010) using Abs: αp50, αRelB (Active Motif, USA); αp65 (Abcam plc., USA); αp52, αcRel and rabbit IgG (Santa Cruz Biotechnology, USA). Bands were visualized using a phosphoimager (Bio-Rad Molecular Imager FX, USA).

Western and dot blotting were performed as described (Bhattacharyya et al., 2004, Toulouse et al., 2005). Blots were probed with Abs specific for: IκBα, IκBβ, IκBε, IKK1, PI3K/p110β and PI3K/p110δ (Santa Cruz Biotechnology, USA); phospho-IκBα, phospho-IKK1/phospho-IKK2 (Ser180/Ser181), IKK2, phospho-AKT (Ser473), AKT, phospho-SAPK/JNK (Thr183/Tyr185), SAPK/JNK, phospho-p38MAPK (Thr180/Tyr182), p38MAPK, phospho-ERK1/phospho-ERK2 (Thr202/Tyr204), ERK1/ERK2, phospho-c-Src (Tyr416), c-Src, phospho-p70S6 Kinase (phospho-p70S6K) (Thr389), p70S6K, phospho-eukaryotic initiation factor 4E binding protein 1 (phospho-

4E-BP1) (Thr37/46), 4E-BP1, phospho-mTOR (Ser2448), mTOR, phospho-glycogen synthase kinase 3β (phospho-GSK3β) (Ser9), GSK3β, influenza hemagglutinin (HA), PI3K/p110α and PI3K/p85α (Cell Signaling Technology, USA); c-Met and phospho-Tyrosine (phospho-Tyr) (Millipore, USA); and β-actin (Sigma-Aldrich, USA). Binding of secondary HRP-labeled goat-αrabbit (Santa Cruz Biotechnology, USA) or goat-αmouse (Sigma-Aldrich, USA) Abs was analyzed using SuperSignal^{R} West Pico or West Dura Chemiluminescent Substrate (Pierce, USA).

2.5. siRNA and DNA transfection of BMDCs

BMDCs were transfected with either a scrambled control set of oligos or siRNAs (60 nM) specific for c-Src, mTOR or PI3K subunits p110α and/or p110δ (Santa Cruz Biotechnology, USA) using Lipofectamine LTX (Invitrogen, USA) as per the manufacturer's instructions. Transfection efficiency was determined by transfecting DCs with fluorescein isothiocyanate (FITC)-conjugated control siRNA, and measuring the frequency of FITC-positive DCs via flow cytometry. Approximately, >80% of BMDCs were transfected under the conditions used.

The expression vector pcDNA3 encoding HA-tagged constitutively active GSK3β, in which regulatory serine 9 (Ser9) was changed to alanine (HA-GSK3β-S9A); and HA-tagged empty pcDNA3 vector (HA-EV) were provided by Dr. Rujun Gong (Brown University, USA) and Dr. Eminy H. Y. Lee (Academia Sinica, Taiwan), respectively (Gong et al., 2008, Chao et al., 2007). BMDC transfection with expression plasmid or empty vector was performed using TransIT-2020 transfection reagent (Mirus, USA)

following the manufacturer's instructions. BMDCs were then subjected to different treatments as specified. Approximately, 70% BMDCs were transfected under the conditions used, which was determined by transfecting BMDCs with pmaxGFP (Lonza Cologne AG, Germany) and measuring the frequency of GFP^+BMDCs via flow cytometry.

2.6. Immunoprecipitation of c-MET-associated protein complexes

For "pull-down" experiments, DCs (10^7) were treated with HGF (60 ng/ml) for varying times, chilled on ice, resuspended in 1 ml of the cell-permeable protein cross-linker dimethyl 3,3-dithiopropionimidate dihydrochloride (Sigma-Aldrich, USA) in PBS (2 mg/ml) and incubated at room temperature for 20 min. In some experiments, DCs were treated with E804 before HGF treatment. Whole cell lysates were prepared and precleared with protein A/G PLUS-Agarose beads (Santa Cruz Biotechnology, USA). c-MET was immunoprecipitated using protein A/G PLUS-Agarose beads precoated with αc-MET Ab. c-MET-associated protein complexes were identified by probing Western blots with Ab specific for c-Src and the PI3K subunits p85α, p110α, p110β and p110δ.

2.7. IKK assay

IKK complex was immunoprecipitated from 700 μg of a whole DC lysate using protein A/G PLUS-agarose beads and αIKK1Ab. The kinase reaction was performed in vitro by incubating IKK signalome-bead complex with IκBα-GST substrate for 60 min at 30°C in kinase buffer containing 20 μl of magnesium/ATP cocktail (Millipore, USA).

Supernatants were collected and IKK kinase activity determined by measuring phosphorylation of IκBα-GST via Western blot using αphospho-IκBα Ab.

2.8. Flow cytometry

The following monoclonal antibodies used for staining were purchased from BD Biosciences (USA): PE-αmouse CD11c, FITC-αmouse CD11b, FITC-αmouse CD40, FITC-αmouse CD86 and FITC-αmouse CD80. Stained cells were analyzed on a FACSCalibur (BD Biosciences, USA) using Cell Quest Pro software.

2.9. Measurement of IL-12 and TNFα secretion from DCs

DCs ($5x10^5$ cells/well) were pretreated or not with HGF (60 ng/ml) for 6 h, washed and stimulated with LPS for additional 24 h. Supernatants were analyzed for IL-12p70 and TNFα secretion in triplicate using ELISA kits (BD Biosciences, USA) following the manufacturer's instructions.

2.10. Statistical analysis

All statistical analyses were conducted by one-way ANOVA using the SigmaPlot 11.0 program. A probability level of ≤ 0.05 was considered significant. Data are represented as mean ± standard error.

3. RESULTS

3.1. HGF binding to c-MET induces inhibition of NF-κB activation in DCs by blocking IKK activity

HGF treatment suppresses APC function and LPS-induced IL-12 secretion of DCs (Okunishi et al., 2005). Since NF-κB is a key regulator of these events, the effect of HGF pretreatment of DCs on NF-κB signaling was investigated. Immature BMDCs ($CD11c^{+}CD8\alpha^{-}$) prepared from BALB/c mice were pretreated with varying concentrations of HGF for 12 h, stimulated with LPS (500 ng/ml), and nuclear NF-κB DNA binding activity assessed via EMSA. BMDCs treated only with LPS exhibited a 7-fold increase in NF-κB DNA binding compared to untreated BMDCs (Fig. 1A). In contrast, pretreatment of BMDCs with increasing concentrations of HGF inhibited, in a dose-dependent manner, LPS-stimulated NF-κB DNA binding (Fig. 1A). However, OCT-1 DNA binding remained unaltered suggesting that inhibition induced by HGF was NF-κB-specific (Fig. 1A). Notably, 60 ng/ml was the lowest concentration of HGF at which LPS-induced NF-κB activation was maximally suppressed (Fig. 1A). Therefore, 60 ng/ml of HGF was used for all subsequent experiments. Even a 1.7-fold higher HGF concentration (100 ng/ml) was used by other group (Beilmann et al., 2000). Temporal analyses demonstrated that maximum inhibition of LPS-induced NF-κB DNA binding was observed when BMDCs were pretreated with HGF for 6 h or more (Fig. 1B). Furthermore, supershift analyses showed that HGF pretreatment inhibited LPS-induced DNA binding of all NF-κB complexes consisting of p50, p65, cRel and RelB (Fig. 1C).

In accordance to EMSA data, BMDC pretreatment with HGF for 6 h and beyond inhibited LPS-stimulated degradation of IκBα, IκBβ and IκBε (Fig. 1D). LPS-stimulated IκBα phosphorylation was also inhibited by HGF pretreatment (Fig. 1E). HGF-induced inhibition of phosphorylation and degradation of IκBs (Fig. 1D and E) could be due to suppression of upstream IKK activity. Indeed, HGF pretreatment of BMDCs significantly inhibited LPS-induced IKK activity (Fig. 1F). However, IKK1 and IKK2 levels were comparable in respective BMDC lysates (Fig. 1F). Similar to BALB/c BMDCs, LPS-stimulated NF-κB DNA binding, IκB degradation and IKK activity were inhibited in sDCs and BMDCs isolated from BALB/c and B6 mice, respectively, upon HGF pretreatment (Supplemental Fig. 1). This suggested that HGF-induced inhibition of NF-κB signaling is not intrinsic to BMDCs or DC genotype. Importantly, stimulation with TNFα, like LPS, failed to induce NF-κB DNA binding and IκBα degradation in BMDCs pretreated with HGF (Fig. 1G and H); which further indicates the ability of HGF to block various signaling pathways those result in NF-κB activation. Unlike the NF-κB pathway, LPS-stimulated activation of the mitogen-activated protein kinase (MAPK) pathway, as measured by phosphorylation of MAPK mediators such as p38MAPK, ERK1/2 and JNK, was unaffected by HGF pretreatment (Fig. 1I-K).

Next, the role for c-MET, which is expressed by DCs (Kurz et al., 2002), in HGF-induced inhibition of NF-κB activation was investigated by analyzing the effect of c-MET blocking with αc-MET Ab. The ability of αc-MET Ab to block c-MET activation was verified by demonstrating that HGF-induced c-MET phosphorylation was inhibited in BMDCs treated with αc-MET but not an isotype control Ab (Fig. 2A). Interestingly, αc-

MET Ab but not isotype control Ab treatment of BMDCs effectively blocked the inhibitory effect of HGF on LPS-induced NF-κB DNA binding, IκB degradation, IκBα phosphorylation and IKK activation (Fig. 2B-E). The latter was assessed by measuring phosphorylation of IKK1 and IKK2 (Fig. 2E). Collectively, these data suggest that HGF via signaling through c-MET selectively inhibits activation of the NF-κB pathway in DCs by blocking IKK activity.

3.2. HGF-induced c-MET signaling induces the sequential activation of c-Src, PI3K, AKT and mTOR in DCs

Studies have demonstrated that NF-κB activation can be negatively regulated by the PI3K/AKT pathway (Guha and Mackman, 2002). Although HGF generally activates PI3K (Dong et al., 2001, Ponzetto et al., 1993), a lack of PI3K activation despite HGF stimulation has also been reported (Oka et al., 2008). Therefore, whether HGF-stimulated c-MET activation induces the PI3K/AKT pathway in DCs was determined by measuring phosphorylation of the PI3K effector, AKT. An increased AKT phosphorylation was observed in both BMDCs and sDCs upon HGF treatment (Fig. 3A and B). However, HGF-induced AKT phosphorylation was blocked in BMDCs pretreated with αc-MET Ab, and PI3K inhibitors Wort or Ly (Fig. 3C and D). Upon HGF binding to c-MET, p85 subunit of PI3K has been reported to interact with the sequence YVHVNATYVNV of c-Met (Ponzetto et al., 1993). Accordingly, the types of PI3K complexes, which become associated with c-MET following HGF treatment of DCs, were determined. Immunoprecipitation of c-MET from whole BMDC lysates showed that c-MET formed complex with the PI3K regulatory subunit p85α, and catalytic subunits p110α and p110δ

but not p100β in HGF-treated versus untreated BMDCs (Fig. 3E). Therefore, HGF treatment induces association of c-MET with PI3K complexes p85α/p110α and p85α/p110δ, and activates the PI3K/AKT pathway in DCs.

Of note, the sequence YVHVNATYVNV of c-MET is also a docking site for c-Src (Ponzetto et al., 1994). Furthermore, c-Src activation following binding of double-stranded RNA by Toll-like receptor 3 (TLR3) is known to activate the PI3K/AKT pathway (Johnsen et al., 2006). Whether HGF-stimulated c-Src activation is required to induce the PI3K/AKT pathway in DCs was therefore investigated. Initially, association of c-Src with c-MET and activation of c-Src in HGF-treated DCs were verified. Immunoprecipitation of c-MET demonstrated an increased c-Src/c-MET complex formation only after HGF treatment (Fig. 3F). In addition, c-Src activation, which was measured by Tyr416 phosphorylation of c-Src as described (Johnsen et al., 2006), was increased in HGF-treated but not untreated BMDCs and sDCs (Fig. 3G and H). HGF-induced c-Src phosphorylation was blocked upon BMDCs pretreatment with E804, a c-Src inhibitor; or αc-MET Ab but not isotype control Ab (Fig. 3I and J). Furthermore, E804 prevented HGF-induced AKT phosphorylation, and association of p85, p110α and p110δ subunits of PI3K with c-MET (Fig. 3K and L). Therefore, HGF-induced association of PI3K with c-MET and activation of the PI3K/AKT pathway requires c-Src activation.

Next, the effect of HGF treatment on activation of mTOR was verified by analyzing phosphorylation of mTOR effectors p70S6K and 4E-BP1. A significant increase in

phosphorylation of p70S6K and 4E-BP1 was observed upon HGF treatment of BMDCs (Fig. 4A and B). These findings indicate that HGF promotes mTOR activation in BMDCs, which was further confirmed by the observation that mTOR phosphorylation was increased upon HGF treatment (Fig. 4C). HGF-induced phosphorylation of p70S6K and 4E-BP1 was blocked by αc-MET but not isotype Ab treatment (Fig. 4D and E). Furthermore, mTOR inhibitor rapamycin blocked HGF-induced phosphorylation of p70S6K and 4E-BP1 but not AKT (Fig. 4F-H). All these 3 phosphorylation events, however, were effectively suppressed by BMDC pretreatment with AKT inhibitor IV (AI-IV) (Fig. 4I-K). These data indicate that HGF-induced AKT phosphorylation precedes mTOR activation. Additionally, HGF-stimulated phosphorylation of p70S6K and 4E-BP1 was inhibited in BMDCs pretreated with E804, or Wort or Ly (Fig. 4L-O). Similar to BMDCs, HGF treatment induced mTOR activation in sDCs (Fig. 4P and Q). Finally, whether GSK3β, another effector of AKT (Gao et al., 2008, Song et al., 2009), participates in HGF-induced signaling in DCs was investigated. Unlike untreated BMDCs, HGF-treated BMDCs exhibited an increased GSK3β phosphorylation at Ser9 (Fig. 5A). The latter represents inactivation of GSK3β kinase activity (Gong et al., 2008). Pretreatment with inhibitor of AKT but not mTOR blocked HGF-induced GSK3β phosphorylation at Ser9 (Fig. 5B and C). In contrast, BMDC transfection with an expression construct encoding HA-tagged constitutively active GSK3β (HA-GSK3β-S9A) but not HA-tagged empty vector (HA-EV) reduced HGF-induced phosphorylation of p70S6K and 4E-BP1 (Fig. 5D and E). The level of HA protein, however, was similar in BMDCs transfected with HA-GSK3β-S9A or HA-EV (Supplemental Fig. 2). Therefore, GSK3β functions downstream of AKT but upstream of mTOR in HGF-

induced signaling in DCs. Together, our results demonstrate that HGF treatment evokes a sequential activation cascade c-Src→PI3K→AKT→mTOR in DCs. Activation of mTOR via the pathway c-Src-PI3K-AKT is dependent on HGF-stimulated inactivation of GSK3β. Furthermore, the PI3K heterodimers, which are induced in DCs due to c-Src activation by HGF, exhibit specific subunit compositions, namely p85α/p110α and p85α/p110δ.

3.3. Activation of the c-Src-PI3K-AKT-mTOR pathway is essential for HGF-induced inhibition of NF-κB signaling in DCs

The role of c-Src-PI3K-AKT-mTOR signaling in HGF-induced inhibition of NF-κB activation was investigated. Accordingly, the effect of pre-exposure of HGF-treated DCs to c-Src inhibitor E804, PI3K inhibitors Wort or Ly, or mTOR inhibitor rapamycin on LPS-stimulated NF-κB signaling was assessed. BMDC pretreatment with E804 blocked the inhibitory effect of HGF on LPS-stimulated NF-κB DNA binding, IκB degradation and IKK activity (Fig. 6A-C). These LPS-induced events were also readily observed when BMDCs were pretreated with PI3K or mTOR inhibitors and then incubated with HGF (Fig. 6D-I). Inhibitors of c-Src, PI3K and mTOR similarly impaired the ability of HGF to inhibit LPS-induced IKK phosphorylation and NF-κB DNA binding in sDCs (Supplemental Fig. 3).

To rule out the possible off-target action of pharmacological inhibitors of c-Src and mTOR, role of c-Src and mTOR in HGF-induced inhibition of NF-κB signaling were further verified by the gene silencing technique. In contrast to scrambled control siRNA,

BMDC transfection with c-Src- or mTOR-specific siRNAs successfully silenced c-Src and mTOR expression, respectively (Fig. 6J); and prevented HGF-induced inhibition of IKK activity and NF-κB DNA binding stimulated by LPS (Fig. 6K and L). Additionally, these inhibitory effects of HGF were significantly reduced in BMDCs transfected with HA-GSK3β-S9A but not HA-EV (Fig. 7).

To test whether HGF-induced p85α/p110α and p85α/p110δ PI3K complexes contributed to activation of mTOR and therefore inhibited NF-κB signaling, the effects of siRNA-mediated blockade of p110α and p110δ expression were investigated. BMDC transfection with p110α- and/or p110δ-specific siRNA reduced expression of these PI3K subunits by ~80% (Fig. 8A). Interestingly, HGF-induced phosphorylation of p70S6K and 4E-BP1, and inhibition of LPS-stimulated IKK phosphorylation and NF-κB DNA binding were partially blocked in BMDCs transfected with p110α- or p110δ-specific but not control siRNA (Fig. 8B-E). In addition, a complete blockade of these HGF-induced effects was observed in BMDCs transfected with a pool of p110α- plus p110δ-specific siRNAs (Fig. 8B-E). Collectively, these data demonstrate that HGF-induced inhibition of NF-κB activation in DCs requires activation of the c-Src-PI3K-AKT-mTOR pathway. The phosphorylation/inactivation of GSK3β by HGF results in inhibition of IKK and NF-κB activation. Furthermore, HGF induction of PI3K complexes p85α/p110α and p85α/p110δ is necessary for activation of mTOR and consequent inhibition of the NF-κB pathway.

3.4. HGF-induced DC inhibition requires activation of the c-Src-PI3K-AKT-mTOR pathway

Next, whether HGF regulates DC activation and that this effect of HGF is mediated through the c-Src-PI3K-AKT-mTOR pathway in a c-MET dependent manner was determined. Accordingly, the effect of HGF pretreatment of BMDCs on LPS-stimulated expression of costimulatory molecules and secretion of proinflammatory cytokines was investigated. Furthermore, whether BMDC pretreatment with either inhibitors of c-Src (E-804), PI3K (Wort or Ly), or mTOR (rapamycin); or αc-MET Ab can block the effect of HGF on these LPS-stimulated events was analyzed. HGF pretreatment inhibited LPS-stimulated upregulation of CD40, CD80 and CD86 expression (Fig. 9A, D and G). In addition, LPS-induced secretion of proinflammatory cytokines such as IL-12p70 and TNFα was inhibited by HGF pretreatment (Fig. 9B, C, E, F, H and I). However, the inhibitory effects of HGF on up-regulation of costimulatory molecules and secretion of proinflammatory cytokines were markedly reduced in BMDCs pretreated with c-Src, PI3K or mTOR inhibitor (Fig. 9). Similarly, these inhibitory effects of HGF were not observed in BMDCs pretreated with αc-MET Ab but not isotype control Ab (Supplemental Fig. 4). Furthermore, BMDCs transfected with c-Src- or mTOR-specific siRNA continued to secrete IL-12p70 upon LPS stimulation despite HGF pretreatment (Supplemental Fig. 5). These data demonstrate that HGF-induced inhibition of DCs requires c-MET-dependent activation of the c-Src-PI3K-AKT-mTOR pathway.

4. DISCUSSION

HGF is believed to be a potent regulator of DC function (Okunishi et al., 2005). In addition, HGF has been shown to induce DC tolerance (Benkhoucha et al.). However, mechanisms involved in the immunoregulation of DCs by HGF have yet to be delineated. The current study has identified the DC signaling events induced upon HGF treatment and demonstrates their roles in targeting the signaling pathways, which are critically required for DC activation. Three major observations were obtained from this study.

First, pretreatment with HGF inhibits activation of the NF-κB pathway in DCs by blocking IKK activity, and IκB phosphorylation and degradation (Fig. 1; Supplemental Fig. 1). Our data are in conflict with earlier reports demonstrating that HGF stimulates NF-κB activation in human prostate cancer, Madin-Darby canine kidney (MDCK) epithelial and MCF-10A breast cell lines (Fan et al., 2009, Fan et al., 2005, Syed et al., 2008). Distinct effects of HGF on NF-κB signaling may be attributed to different cell types (primary cells such as murine DCs versus human prostate cancer, MDCK epithelial and MCF-10A breast cell lines) used in these studies (Fan et al., 2009, Fan et al., 2005, Syed et al., 2008) opposed to ours. Unlike NF-κB signaling, LPS-induced activation of other signaling pathways, which are known to regulate DC activation/maturation, remains unaffected by HGF treatment. For instance, LPS-induced phosphorylation of the MAPK molecules p38MAPK, ERK1/2 and JNK was not altered despite HGF pretreatment of DCs (Fig. 1I-K). In contrast, HGF-regulated activation of these MAPK mediators has been reported for other cell types (Rush et al., 2007, Awasthi and King, 2000). Therefore, selective impairment of NF-κB activation by HGF appears to be DC-specific. Studies

demonstrated that blockade of NF-κB activation alone can prevent DC activation/maturation (Rescigno et al., 1998, Weaver et al., 2001). Strikingly, HGF-induced inhibition of the NF-κB pathway correlated with suppression of DC activation (Fig. 1; Supplemental Figs. 1 and 4). Our findings coupled with these reports indicate that blockade of NF-κB activation by HGF results in DC suppression.

The second important observation made in this study is that HGF-induced c-Src activation blocks activation of the NF-κB pathway and consequently inhibits DC activation (Figs 3, 6 and 9; Supplemental Figs. 3 and 5). In contrast to this finding, a previous study demonstrates that HGF-induced c-Src activation positively regulates NF-κB activation in human prostate cancer and MDCK epithelial cell lines (Fan et al., 2009). The inhibitory effect of HGF-induced c-Src activation on NF-κB signaling is therefore likely to be DC-specific. Notably, HGF treatment of DCs induces physical association of c-Src with c-MET (Fig. 3F). Although c-Src activation is important for HGF-c-MET-mediated cell migration, transformation and protection (Rahimi et al., 1998, Fan et al., 2009), its role in HGF-regulated DC activation is yet to be defined. Our observations suggest an essential role for c-Src in HGF-induced DC suppression. Since activation of c-Src is considered as one of the proximal signaling events induced by c-MET after HGF binding (Ponzetto et al., 1994), c-Src activation would be expected to block NF-κB signaling by regulating activation of downstream signaling molecules. Importantly, TLR3-mediated c-Src activation is reported to activate PI3K (Johnsen et al., 2006). Therefore, one intriguing possibility was that c-Src activation might induce the PI3K/AKT pathway in HGF-treated DCs. Indeed, c-Src activation was found essential for

association of PI3K with c-MET and induction of the PI3K/AKT pathway in DCs treated with HGF (Fig. 3K and L). Until now, involvement of the PI3K/AKT pathway in immunoregulation of DCs by HGF remains unknown. Accordingly, a role for the PI3K/AKT pathway in HGF-induced inhibition of NF-κB signaling and DC activation was determined by the use of PI3K inhibitors Wort and Ly. Pretreatment with Wort or Ly effectively blocked the capacity of HGF to inhibit LPS-stimulated NF-κB signaling and DC activation (Figs 6D-F and 9D-F; Supplemental Fig. 3). This suggests that these inhibitory effects of HGF are mediated through the PI3K/AKT pathway.

Our third finding is that induction of specific PI3K complexes p85α/p110α and p85α/p110δ is required for inhibition of NF-κB signaling by HGF in DCs. Indeed, the inhibitory effects of HGF on LPS-induced NF-κB signaling were blocked by DC transfection with siRNAs specific for p110α and p110δ subunits (Fig. 8). Importantly, PI3K can inhibit both LPS-induced activation of p38MAPK and NF-κB (Fukao et al., 2002, Guha and Mackman, 2002). The inhibitory effect of PI3K activation on a specific pathway may be determined by the types of PI3K complexes induced upon cellular stimulation. For example, p85α/p110β complex mediates the inhibitory effect of PI3K on LPS-stimulated p38MAPK activation in DCs (Fukao et al., 2002). In contrast, HGF induction of p85α/p110α and p85α/p110δ complexes does not affect p38MAPK activation but prevents activation of NF-κB signaling in DCs treated with LPS (Figs 1, 3E and 8).

Noteworthy is that HGF-induced p85α/p110α and p85α/p110δ PI3K complexes inhibit LPS-stimulated NF-κB pathway and DC activation by activating mTOR. This conclusion is supported by two findings. First, mTOR activation was significantly inhibited in DCs transfected with p110α- or/and p110δ-specific siRNAs despite HGF stimulation (Fig. 8B and C). Second, LPS continued to induce NF-κB signaling and DC activation when HGF-stimulated mTOR activation was blocked (Figs. 6 and 9; Supplemental Figs. 3 and 5). The latter findings are in accordance with a recent report indicating a negative regulation of NF-κB activation by mTOR in human monocytes (Weichhart et al., 2008). Importantly, Weichhart et al. reported that mTOR negatively modulates activity of transactivation domain of NF-κB/p65 subunit to dampen NF-κB activation (Weichhart et al., 2008). However, the fact that NF-κB nuclear translocation is impaired in $TSC2^{-/-}$ cells (Weichhart et al., 2008), implicates a possible role for mTOR in regulating upstream events of the NF-κB pathway. Indeed, our results demonstrate that the increased mTOR activation by HGF blocks LPS-stimulated IKK activity and IκB degradation in DCs (Figs. 4 and 6; Supplemental Fig. 3). The precise mechanism for mTOR-mediated suppression of IKK activation in HGF-treated DCs is still unclear and currently under investigation. Nevertheless, our findings suggest that blockade of IKK activation by mTOR is required for HGF-induced suppression of the NF-κB pathway and DC activation. Whereas HGF has been shown to activate mTOR in MCF-10A breast cell line, its role in HGF-induced NF-κB activation was not examined (Syed et al., 2008). Furthermore, blockade of mTOR activation has minimal effect on HGF-induced NF-κB activation in human prostate cancer and MDCK epithelial cell lines, although HGF-induced NF-κB activation in these cells is AKT-dependent (Fan et al., 2005, Fan et al.,

2009). In contrast, our study establishes a direct role for mTOR in HGF-induced suppression of NF-κB signaling and subsequent DC activation, which remained unknown so far. This disparity underscores the relative importance of mTOR activation in HGF regulation of NF-κB signaling in DCs versus other cell types.

A recent report using human renal epithelial cell line demonstrates that HGF induces phosphorylation/inactivation of GSK3β, which blocks NF-κB DNA binding but not NF-κB nuclear translocation or IκB degradation (Gong et al., 2008). Furthermore, GSK3β$^{-/-}$ cells exhibit a reduced NF-κB DNA binding compared to wild-type cells, although GSK3β deficiency does not affect IκB degradation and NF-κB nuclear translocation (Hoeflich et al., 2000). Importantly, GSK3β regulates NF-κB activity at the level of transcriptional complex (Hoeflich et al., 2000). In marked contrast, our results demonstrate that HGF inhibits NF-κB activation by blocking IKK activation and IκB degradation, although HGF-induced GSK3β phosphorylation is observed in DCs (Figs. 1 and 5; Supplemental Fig. 1). Furthermore, ectopic expression of constitutively active GSK3β (Supplemental Fig. 6) reduces the inhibitory effect of HGF on both IKK and NF-κB activation in DCs (Fig. 7). Therefore, it is likely that HGF-induced GSK3β phosphorylation indirectly suppresses NF-κB activation in DCs by promoting activation of mTOR, a downstream mediator of GSK3β (Fig. 5) (Buller et al., 2008, Inoki et al., 2006), and that the mechanism by which HGF suppresses NF-κB activity is dependent on the cell type.

A potential implication of this study pertains to the immunotherapy for multiple myeloma (MM). In MM patients, the increase in serum HGF levels correlates with unfavorable prognosis (Seidel et al., 2002). The antitumor efficacy of DC-based immunotherapy may be compromised due to HGF-induced impairment of DC function (Rutella et al., 2006a). From therapeutic point of view, an understanding of the molecular events involved in HGF-induced suppression of DCs is critically important. The present study has identified the c-Src→PI3K→AKT→mTOR pathway, which plays an essential role in HGF-induced inhibition of DC activation by blocking NF-κB signaling. Furthermore, induction of specific PI3K complexes p85α/p110α and p85α/p110δ is required for inhibition of the NF-κB pathway by HGF. The latter finding is noteworthy in view of a very recent report suggesting PI3K/p110δ as a novel therapeutic target for MM (Ikeda et al., 2010). Importantly, an abundant expression of PI3K/p110α in majority of human MM cell lines has also been reported (Ikeda et al., 2010).

In conclusion, the current study defines the molecular basis for HGF-induced DC inhibition by demonstrating a pivotal role for the c-Src-PI3K-AKT-mTOR pathway in this process. Targeting these signaling molecules may provide an approach for restoration of the efficacy of DC-based antitumor immunotherapy by preventing HGF-induced DC dysfunction.

Acknowledgement

E.S. is a recipient of fellowship from University Grant Commission, Government of India. This study was supported by grant from the Department of Biotechnology, Government of India and intramural grant from the Council for Scientific and Industrial Research, Government of India (P.S.). We thank Dr. Rujun Gong (Brown University School of Medicine, Providence, Rhode Island, USA) and Dr. Eminy H. Y. Lee (Institute of Biomedical Sciences, Academia Sinica, Taiwan) for providing HA-GSK3β-S9A/pcDNA3 and HA/pcDNA3 vectors, respectively. Finally, we thank IMTECH animal house facility for providing animals required for experimentation.

REFERENCES

Awasthi V, King RJ. PKC, p42/p44 MAPK, and p38 MAPK are required for HGF-induced proliferation of H441 cells. Am J Physiol Lung Cell Mol Physiol 2000;279:L942-9.

Beg AA, Finco TS, Nantermet PV, Baldwin Jr AS. Tumor necrosis factor and interleukin-1 lead to phosphorylation and loss of IkappaB alpha: a mechanism for NF-kappaB activation. Mol Cell Biol 1993;13:3301-10.

Beilmann M, Vande Woude GF, Dienes HP, Schirmacher P. Hepatocyte growth factor-stimulated invasiveness of monocytes. Blood 2000;95:3964-9.

Benkhoucha M, Santiago-Raber ML, Schneiter G, Chofflon M, Funakoshi H, Nakamura T, et al. Hepatocyte growth factor inhibits CNS autoimmunity by inducing tolerogenic dendritic cells and CD25+Foxp3+ regulatory T cells. Proc Natl Acad Sci USA 2010;107:6424-9.

Bhattacharyya S, Sen P, Wallet M, Long B, Baldwin Jr AS, Tisch R. Immunoregulation of dendritic cells by IL-10 is mediated through suppression of the PI3K/Akt pathway and of IkappaB kinase activity. Blood 2004;104:1100-9.

Buller CL, Loberg RD, Fan MH, Zhu Q, Park JL, Vesely E, et al. A GSK-3/TSC2/mTOR pathway regulates glucose uptake and GLUT1 glucose transporter expression. Am J Physiol Cell Physiol 2008;295:C836-43.

Chao CC, Ma YL, Lee EH. Protein kinase CK2 impairs spatial memory formation through differential cross talk with PI-3 kinase signaling: activation of Akt and inactivation of SGK1. J Neurosci 2007;27:6243-8.

Dong G, Chen Z, Li ZY, Yeh NT, Bancroft CC, Van Waes C. Hepatocyte growth factor/scatter factor-induced activation of MEK and PI3K signal pathways contributes to expression of proangiogenic cytokines interleukin-8 and vascular endothelial growth factor in head and neck squamous cell carcinoma. Cancer Res 2001;61:5911-8.

Fan S, Gao M, Meng Q, Laterra JJ, Symons MH, Coniglio S, et al. Role of NF-kappaB signaling in hepatocyte growth factor/scatter factor-mediated cell protection. Oncogene 2005;24:1749-66.

Fan S, Meng Q, Laterra JJ, Rosen EM. Role of Src signal transduction pathways in scatter factor-mediated cellular protection. J Biol Chem 2009;284:7561-77.

Fukao T, Tanabe M, Terauchi Y, Ota T, Matsuda S, Asano T, et al. PI3K-mediated negative feedback regulation of IL-12 production in DCs. Nat Immunol 2002;3:875-81.

Gao X, Zhang H, Takahashi T, Hsieh J, Liao J, Steinberg GK, et al. The Akt signaling pathway contributes to postconditioning's protection against stroke; the protection is associated with the MAPK and PKC pathways. J Neurochem 2008;105:943-55.

Ghosh S, Karin M. Missing pieces in the NF-kappaB puzzle. Cell 2002;109 Suppl:S81-96.

Gong R, Rifai A, Ge Y, Chen S, Dworkin LD. Hepatocyte growth factor suppresses proinflammatory NF-kappaB activation through GSK3beta inactivation in renal tubular epithelial cells. J Biol Chem 2008;283:7401-10.

Guha M, Mackman N. The phosphatidylinositol 3-kinase-Akt pathway limits lipopolysaccharide activation of signaling pathways and expression of inflammatory mediators in human monocytic cells. J Biol Chem 2002;277:32124-32.

Haldar AK, Yadav V, Singhal E, Bisht KK, Singh A, Bhaumik S, et al. Leishmania donovani isolates with antimony-resistant but not -sensitive phenotype inhibit

sodium antimony gluconate-induced dendritic cell activation. PLoS Pathog 2010;6:e1000907.

Hilkens CM, Kalinski P, de Boer M, Kapsenberg ML. Human dendritic cells require exogenous interleukin-12-inducing factors to direct the development of naive T-helper cells toward the Th1 phenotype. Blood 1997;90:1920-6.

Hoeflich KP, Luo J, Rubie EA, Tsao MS, Jin O, Woodgett JR. Requirement for glycogen synthase kinase-3beta in cell survival and NF-kappaB activation. Nature 2000;406:86-90.

Ikeda H, Hideshima T, Fulciniti M, Perrone G, Miura N, Yasui H, et al. PI3K/p110{delta} is a novel therapeutic target in multiple myeloma. Blood 2010;116:1460-8.

Inoki K, Ouyang H, Zhu T, Lindvall C, Wang Y, Zhang X, et al. TSC2 integrates Wnt and energy signals via a coordinated phosphorylation by AMPK and GSK3 to regulate cell growth. Cell 2006;126:955-68.

Johnsen IB, Nguyen TT, Ringdal M, Tryggestad AM, Bakke O, Lien E, et al. Toll-like receptor 3 associates with c-Src tyrosine kinase on endosomes to initiate antiviral signaling. EMBO J 2006;25:3335-46.

Jonuleit H, Schmitt E, Schuler G, Knop J, Enk AH. Induction of interleukin 10-producing, nonproliferating CD4(+) T cells with regulatory properties by repetitive stimulation with allogeneic immature human dendritic cells. J Exp Med 2000;192:1213-22.

Kurz SM, Diebold SS, Hieronymus T, Gust TC, Bartunek P, Sachs M, et al. The impact of c-met/scatter factor receptor on dendritic cell migration. Eur J Immunol 2002;32:1832-8.

Nakamura T, Nawa K, Ichihara A. Partial purification and characterization of hepatocyte growth factor from serum of hepatectomized rats. Biochem Biophys Res Commun 1984;122:1450-9.

Oka M, Kikkawa U, Nishigori C. Protein kinase C-betaII represses hepatocyte growth factor-induced invasion by preventing the association of adapter protein Gab1 and phosphatidylinositol 3-kinase in melanoma cells. J Invest Dermatol 2008;128:188-95.

Okunishi K, Dohi M, Nakagome K, Tanaka R, Mizuno S, Matsumoto K, et al. A novel role of hepatocyte growth factor as an immune regulator through suppressing dendritic cell function. J Immunol 2005;175:4745-53.

Ponzetto C, Bardelli A, Maina F, Longati P, Panayotou G, Dhand R, et al. A novel recognition motif for phosphatidylinositol 3-kinase binding mediates its association with the hepatocyte growth factor/scatter factor receptor. Mol Cell Biol 1993;13:4600-8.

Ponzetto C, Bardelli A, Zhen Z, Maina F, dalla Zonca P, Giordano S, et al. A multifunctional docking site mediates signaling and transformation by the hepatocyte growth factor/scatter factor receptor family. Cell 1994;77:261-71.

Rahimi N, Hung W, Tremblay E, Saulnier R, Elliott B. c-Src kinase activity is required for hepatocyte growth factor-induced motility and anchorage-independent growth of mammary carcinoma cells. J Biol Chem 1998;273:33714-21.

Rescigno M, Martino M, Sutherland CL, Gold MR, Ricciardi-Castagnoli P. Dendritic cell survival and maturation are regulated by different signaling pathways. J Exp Med 1998;188:2175-80.

Rush S, Khan G, Bamisaiye A, Bidwell P, Leaver HA, Rizzo MT. c-jun amino-terminal kinase and mitogen activated protein kinase 1/2 mediate hepatocyte growth factor-induced migration of brain endothelial cells. Exp Cell Res 2007;313:121-32.

Rutella S, Bonanno G, Procoli A, Mariotti A, de Ritis DG, Curti A, et al. Hepatocyte growth factor favors monocyte differentiation into regulatory interleukin (IL)-10++IL-12low/neg accessory cells with dendritic-cell features. Blood 2006a;108:218-27.

Rutella S, Danese S, Leone G. Tolerogenic dendritic cells: cytokine modulation comes of age. Blood 2006b;108:1435-40.

Seidel C, Lenhoff S, Brabrand S, Anderson G, Standal T, Lanng-Nielsen J, et al. Hepatocyte growth factor in myeloma patients treated with high-dose chemotherapy. Br J Haematol 2002;119:672-6.

Song JQ, Teng X, Cai Y, Tang CS, Qi YF. Activation of Akt/GSK-3beta signaling pathway is involved in intermedin(1-53) protection against myocardial apoptosis induced by ischemia/reperfusion. Apoptosis 2009;14:1299-307.

Syed DN, Afaq F, Sarfaraz S, Khan N, Kedlaya R, Setaluri V, et al. Delphinidin inhibits cell proliferation and invasion via modulation of Met receptor phosphorylation. Toxicol Appl Pharmacol 2008;231:52-60.

Toulouse A, Au-Yeung F, Gaspar C, Roussel J, Dion P, Rouleau GA. Ribosomal frameshifting on MJD-1 transcripts with long CAG tracts. Hum Mol Genet 2005;14:2649-60.

Ueki T, Kaneda Y, Tsutsui H, Nakanishi K, Sawa Y, Morishita R, et al. Hepatocyte growth factor gene therapy of liver cirrhosis in rats. Nat Med 1999;5:226-30.

van der Voor R, Taher TE, Keehnen RM, Smit L, Groenink M, Pals ST. Paracrine regulation of germinal center B cell adhesion through the c-met-hepatocyte growth factor/scatter factor pathway. J Exp Med 1997;185:2121-31.

Weaver Jr DJ, Poligone B, Bui T, Abdel-Motal UM, Baldwin Jr AS, Tisch R. Dendritic cells from nonobese diabetic mice exhibit a defect in NF-kappaB regulation due to a hyperactive IkappaB kinase. J Immunol 2001;167:1461-8.

Weichhart T, Costantino G, Poglitsch M, Rosner M, Zeyda M, Stuhlmeier KM, et al. The TSC-mTOR signaling pathway regulates the innate inflammatory response. Immunity 2008;29:565-77.

Yamaura K, Ito K, Tsukioka K, Wada Y, Makiuchi A, Sakaguchi M, et al. Suppression of acute and chronic rejection by hepatocyte growth factor in a murine model of cardiac transplantation: induction of tolerance and prevention of cardiac allograft vasculopathy. Circulation 2004;110:1650-7.

Zarnegar R, Michalopoulos GK. The many faces of hepatocyte growth factor: from hepatopoiesis to hematopoiesis. J Cell Biol 1995;129:1177-80.

FIGURE LEGENDS

Figure 1. Pretreatment with HGF inhibits activation of the NF-κB but not MAPK pathway in BMDCs.

BALB/c BMDCs were pretreated either with varying concentrations of HGF for 12 h (A) or 60 ng/ml of HGF for indicated times (B-K) or left untreated. BMDCs were then stimulated with LPS for 30 min. In some experiments (G and H), BMDCs were stimulated with TNFα for 1 h after HGF treatment. (A and B) Nuclear DNA binding activity of NF-κB was measured via EMSA. DNA binding activity of OCT-1 was used as an internal control. Densitometric analyses were determined by measuring the ratio of intensity of NF-κB to OCT-1 binding per unit area and represented as arbitrary units. (C) DNA binding of different NF-κB complexes was determined by supershift analysis using rabbit IgG (Control Ab) or Abs specific for different NF-κB subunits. (D, H) Expression of IκBα, IκBβ, IκBε and β-actin protein in cytoplasmic extracts was determined via Western blot using the same blots. (E) Cytoplasmic phospho (P)-IκBα expression was determined by Western blot. The same blot was reprobed for β-actin. (F) In vitro IKK activity was determined by measuring phosphorylation of an IκBα-GST substrate. IKK1 and IKK2 protein expression in immunoprecipitated samples were analyzed via Western blot. (G) Nuclear NF-κB or OCT-1 DNA binding activity was determined via EMSA. (I-K) Expression of phospho-p38MAPK versus p38MAPK (I), phospho-ERK versus ERK (J) and phospho-JNK versus JNK (K) in whole cell lysates was determined via Western blot with the same blots. For this and all other figures, control (Cont) lane represents DCs without HGF treatment or any stimulation (e.g. LPS or TNFα); and the lane HGF represents DCs treated with HGF in the absence of any stimulation. For all experiments,

DCs derived from BALB/c mice were used unless DCs of other mouse strain are specified. Data are representative of 3 independent experiments.

Figure 2. Blockade of c-MET activation with αc-MET Ab prevents HGF-induced inhibition of NF-κB activation in BMDCs. BMDCs pretreated with αc-MET or isotype control Ab were incubated with HGF (60 ng/ml) for indicated times. For some experiments (B-E), BMDCs were stimulated with LPS for 30 min after HGF treatment. (A) c-MET was immunoprecipitated from whole cell-lysates and Western blots were probed for phospho-Tyrosine [(P)-Tyr] and c-MET using the same membranes. (B) Nuclear NF-κB or OCT-1 DNA binding activity was determined via EMSA. (C) Cytoplasmic IκBα, IκBβ, IκBε and β-actin protein were detected via Western blot with same blot. (D) Phospho-IκBα was detected by Western blot. The same blot was reprobed for β-actin. (E) Expression of phospho-IKK1/2 versus IKK1 and IKK2 in the cytoplasmic extract was determined via Western blot. Data are representative of 3 independent experiments.

Figure 3. HGF induces the sequential activation of c-Src and the PI3K/AKT pathway in DCs. BMDCs (A, C-G and I-L) and sDCs (B and H) were treated with HGF (60 ng/ml) for indicated times. For experiments (C, D and I-L), DCs were incubated with αc-MET or isotype control Ab (C and J), PI3K inhibitors Wort or Ly (D), or c-Src inhibitor E804 (I, K and L) prior to HGF treatment. (A-D and K) Phosphorylation of AKT in cytoplasmic extracts was determined via Western blot using αphospho-AKT Ab. The same blot was reprobed for AKT protein. (E, F and L) c-MET was

immunoprecipitated from whole cell-lysates and Western blots were probed for PI3K subunits p85α, p110α, p110β and p110δ (E and L), c-Src (F), and c-MET (E, F and L). (G-J) Western blot was used to detect phospho-c-Src versus c-Src in whole cell lysates with the same blots. Data are representative of 3 independent experiments.

Figure 4. HGF binding to c-MET activates mTOR as a downstream activation event of c-Src-PI3K-AKT signaling cascade. BMDCs (A-O) and sDCs (P and Q) were incubated with HGF (60 ng/ml) for indicated times. In some experiments (D-O), DCs were pretreated with isotype control Ab or αc-MET Ab (D and E), mTOR inhibitor rapamycin (F-H), AKT inhibitor AI-IV (I-K), c-Src inhibitor E804 (L and M), or PI3K inhibitors Wort or Ly (N and O) prior to HGF treatment or left untreated. Whole cell lysates were prepared to detect phospho-p70S6K versus p70S6K (A, D, F, J, L, N and P), phospho-4E-BP1 versus 4E-BP1 (B, E, G, K, M, O and Q), phospho-mTOR versus mTOR (C), and phospho-AKT versus AKT (H and I) via Western blot with the same blots. Data are representative of 3 independent experiments.

Figure 5. GSK3β operates downstream of AKT but upstream of mTOR in HGF signaling. BMDCs were treated with HGF (60 ng/ml) for indicated times. For some experiments (B-E), BMDCs were either incubated with AKT inhibitor AI-IV (B), or mTOR inhibitor rapamycin (C); or transfected with specified concentrations of HA-tagged empty pcDNA3 vector (HA-EV) or pcDNA3 vector encoding HA-conjugated constitutively active GSK3β (HA-GSK3β-S9A) prior to HGF treatment (D and E). Expression of phospho-GSK3β versus GSK3β (A-C), phospho-p70S6K versus p70S6K

(D) and phospho-4E-BP1 versus 4E-BP1 (E) in whole cell lysates was detected via Western blot with the same blots. Data are representative of 3 independent experiments.

Figure 6. c-Src, PI3K and mTOR activation are required for HGF-induced inhibition of NF-κB signaling in BMDCs. BMDCs were incubated or not with E804 (A-C); Wort or Ly (D-F); or rapamycin (G-I). Alternatively, BMDCs were transfected with scrambled control siRNA or siRNAs specific for c-Src or mTOR (J-L). BMDCs were then treated with HGF (60 ng/ml) for 6 h and stimulated with LPS for 30 min. (A, D, G and L) DNA binding activity of nuclear NF-κB and OCT-1 was determined via EMSA. (B, E, and H) Cytoplasmic IκBα, IκBβ, IκBε and β-actin were detected via Western blot using the same blots. (C, F, I and K) In vitro IKK activity and expression of IKK1 and IKK2 were determined as in Figure 1. (J) Expression of c-Src, mTOR and β-actin in whole cell lysates was detected via Western blot with the same membrane. Data are representative of 3 independent experiments.

Figure 7. Ectopic expression of constitutively active GSK3β impairs HGF-induced inhibition of IKK and NF-κB activation in BMDCs. BMDCs were transfected or not with 5 μg of HA-tagged empty pcDNA3 vector (HA-EV) or pcDNA3 vector expressing HA-conjugated constitutively active GSK3β (HA-GSK3β-S9A), incubated with HGF (60 ng/ml) for 6 h and stimulated with LPS for 30 min. In vitro IKK activity and expression of IKK1 and IKK2 were determined as in Figure 1. (A), and nuclear NF-κB or OCT-1 DNA binding activity was determined via EMSA (B). Data are representative of 3 independent experiments.

Figure 8. PI3K complexes p85α/p110α and p85α/p110δ mediate HGF-induced activation of mTOR and inhibition of NF-κB signaling. (A) BMDCs were transfected with either scrambled control siRNA or siRNAs specific for p110α or/and p110δ subunits of PI3K. Expression of p110α, p110δ and β-actin was detected via Western blot with the same membrane. (B and C) BMDCs transfected with scrambled control siRNA and/or siRNAs specific for p110α or/and p110δ were incubated with HGF (60 ng/ml) for 6 h or left untreated. Cytoplasmic expression of phospho-p70S6K versus p70S6K (B), and phospho-4E-BP1 versus 4E-BP1 (C) was determined via Western blot using the same membranes. (D and E) BMDCs transfected with different siRNAs as mentioned above were incubated with HGF (60 ng/ml) for 6 h and stimulated with LPS for 30 min. Phospho-IKK1/2, IKK1 and IKK2 were detected in whole cell lysates via Western blot using the same membranes (D), or DNA binding activity of nuclear NF-κB or OCT-1 was determined via EMSA (E). Data are representative of 3 independent experiments.

Figure 9. HGF-induced inhibition of BMDC activation requires activation of c-Src, PI3K and mTOR. BMDCs were pretreated or not with E804 (A-C); Wort or Ly (D-F); or rapamycin (G-I). Subsequently, BMDCs were incubated with HGF (60 ng/ml) for 6 h and stimulated with LPS for 48 (A, D and G) or 24 h (B, C, E, F, H and I). (A, D and G) Surface expression of costimulatory molecules was measured via FACS. (B, C, E, F, H and I) Secretion of IL-12p70 (B, E and H) and TNFα (C, F and I) in culture supernatants were measured via ELISA. Data are the representative of 3 independent experiments and were analyzed using one-way ANOVA. $^{*}p < 0.001$ DC+E804+HGF+LPS,

DC+Wort+HGF+LPS, DC+Ly+HGF+LPS or DC+Rapamycin+HGF+LPS versus DC+HGF+LPS.

Figure-1

Click here to download high resolution image

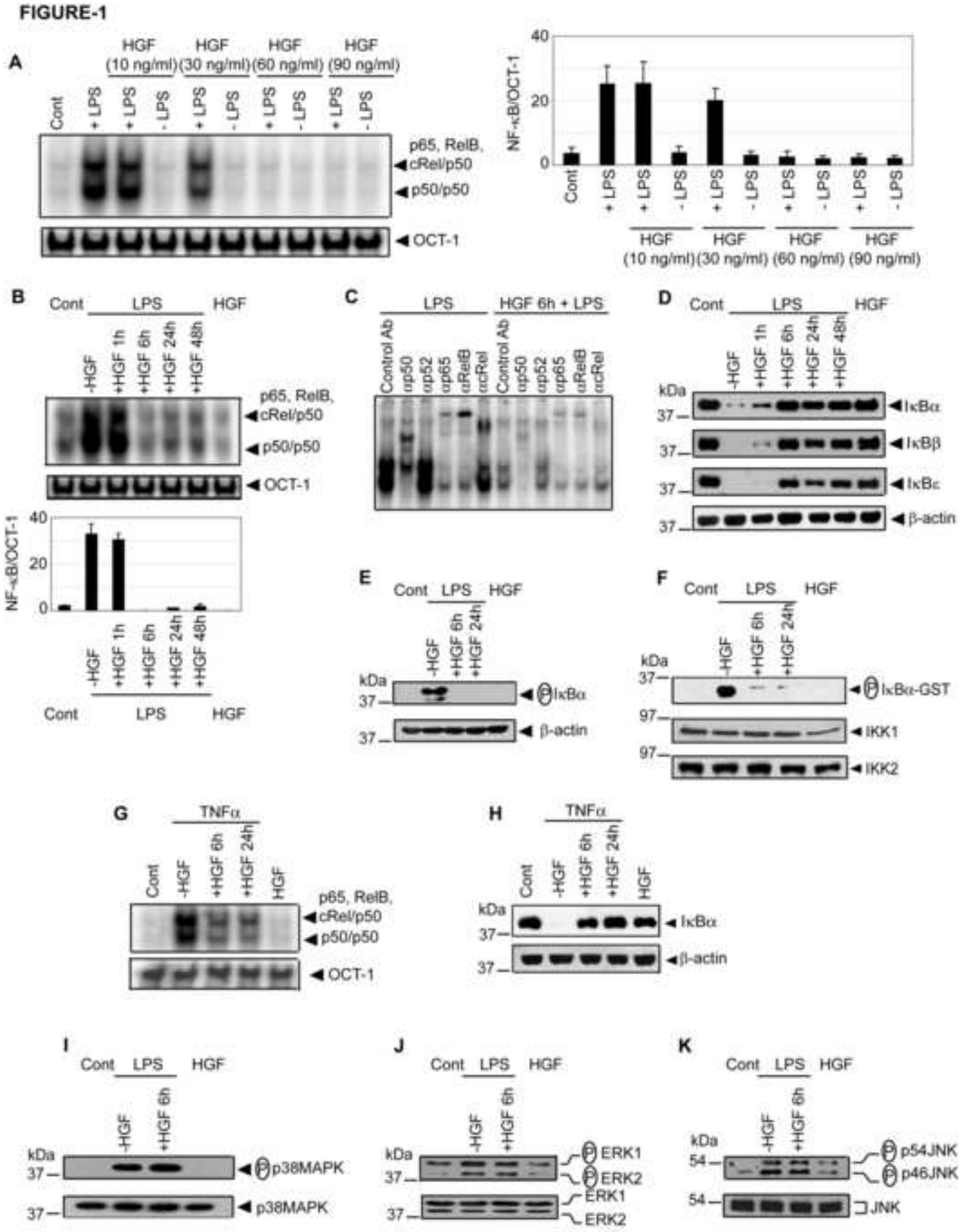

Figure-2

Click here to download high resolution image

FIGURE-2

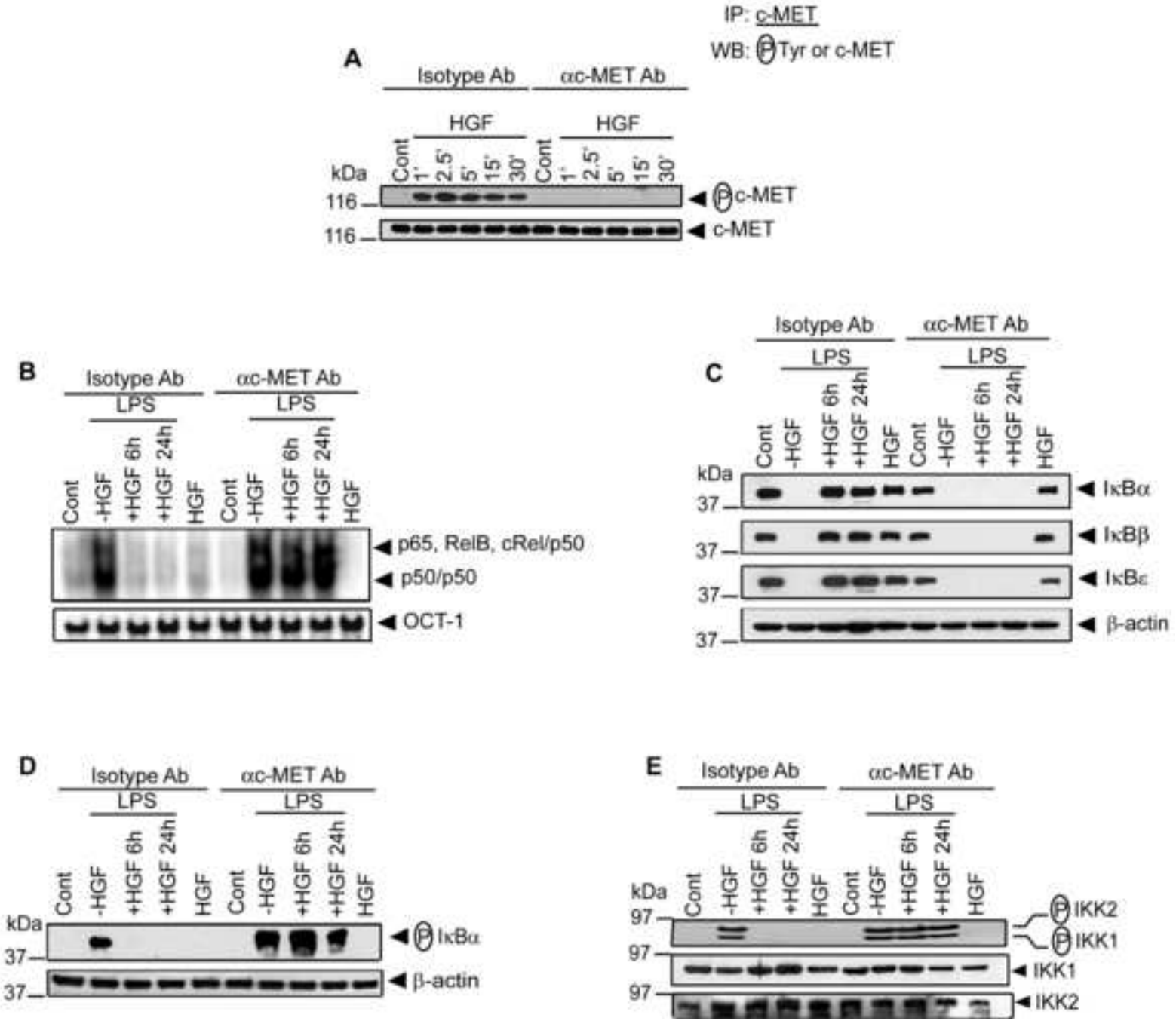

Figure-3

Click here to download high resolution image

FIGURE-3

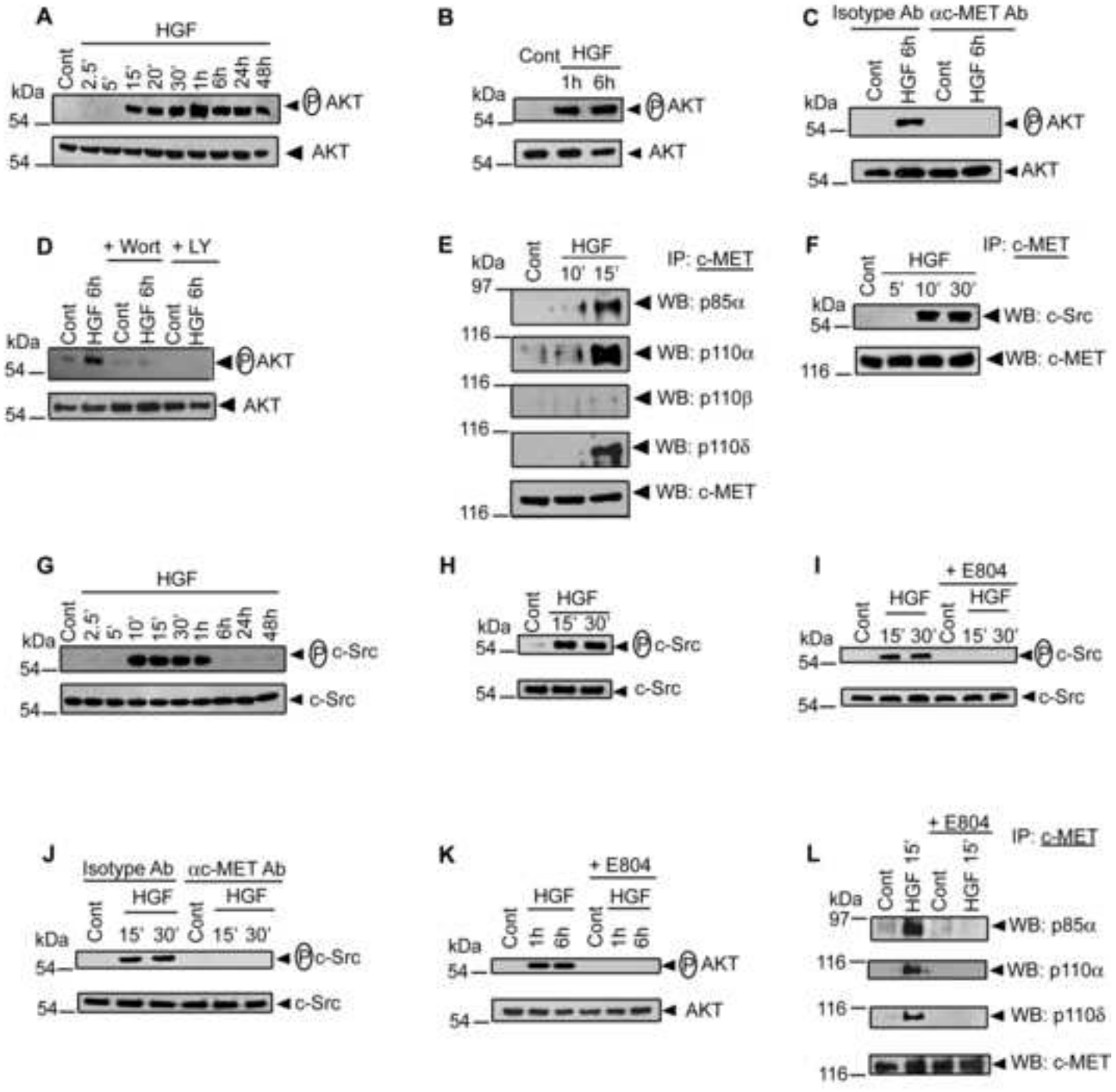

Figure-4

Click here to download high resolution image

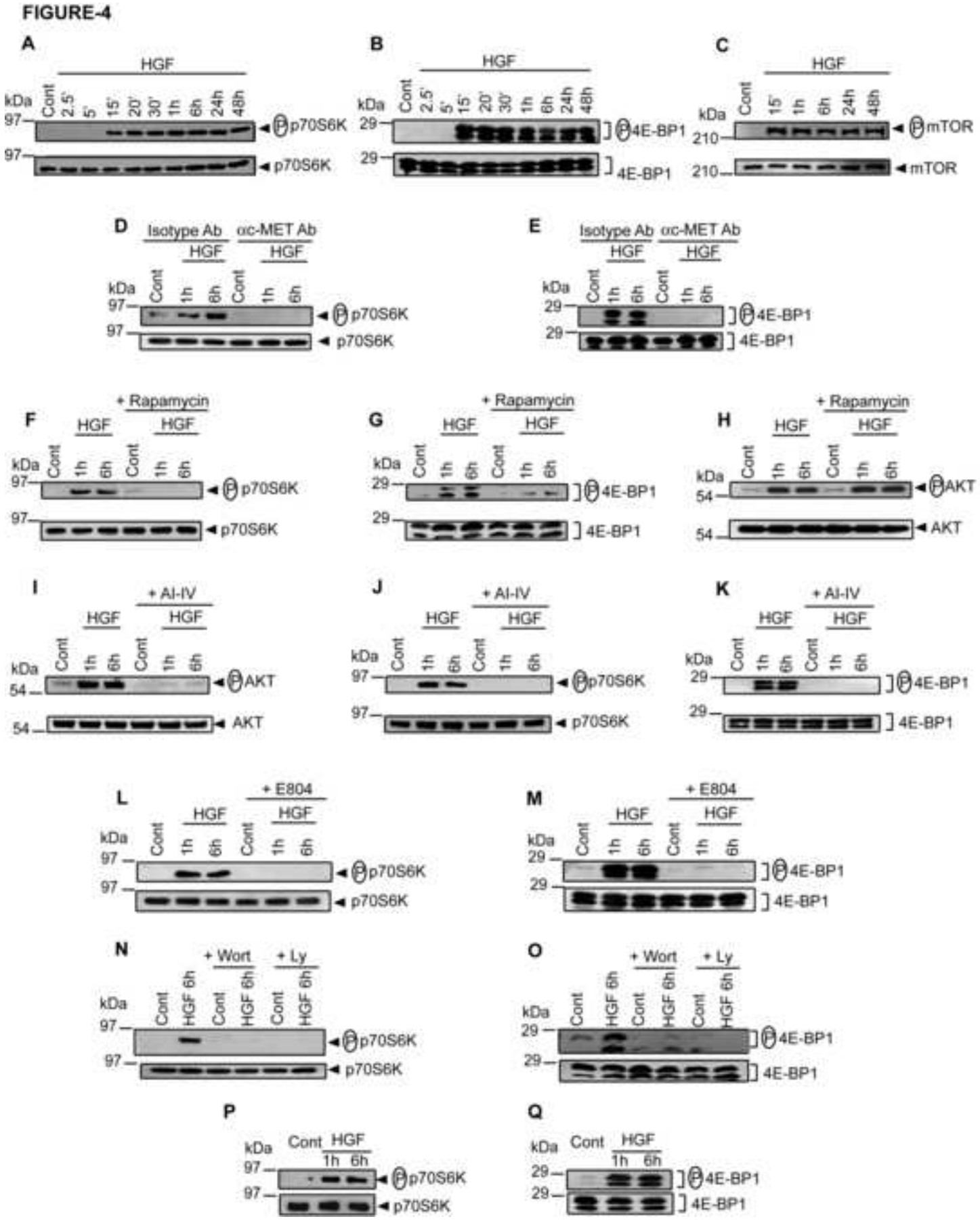

Figure-5
Click here to download high resolution image

FIGURE-5

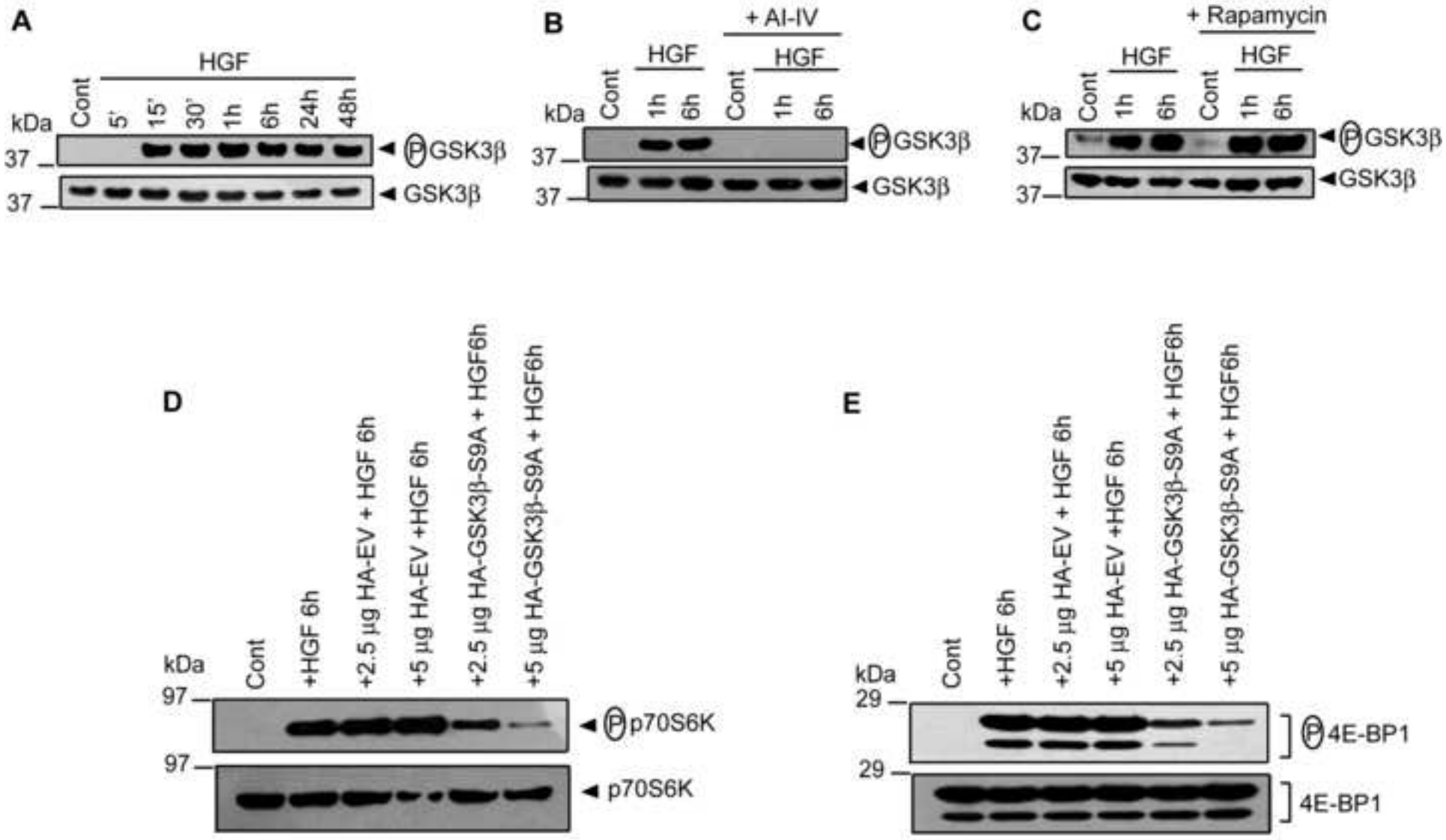

Figure-6

Click here to download high resolution image

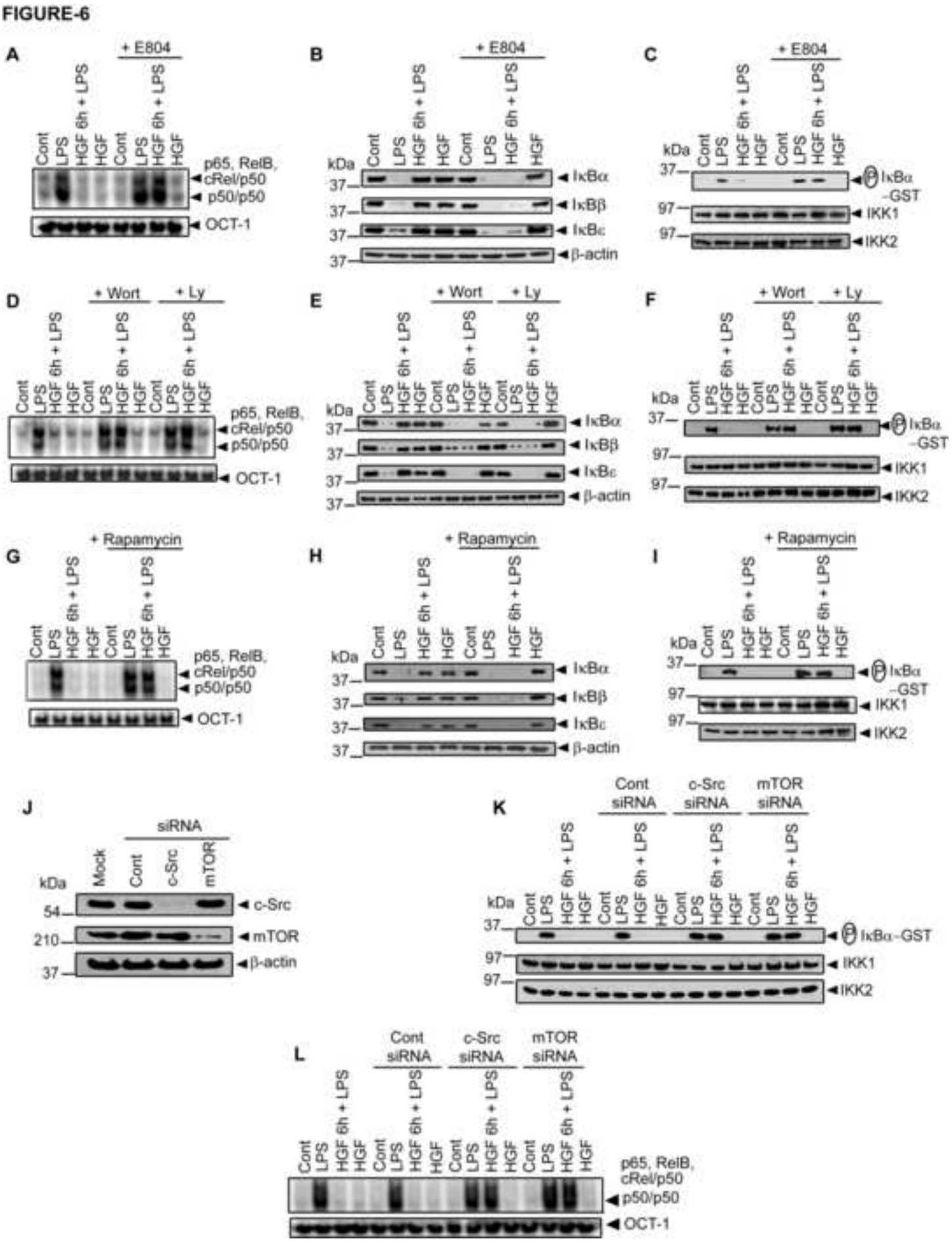

Figure-7
Click here to download high resolution image

FIGURE-7

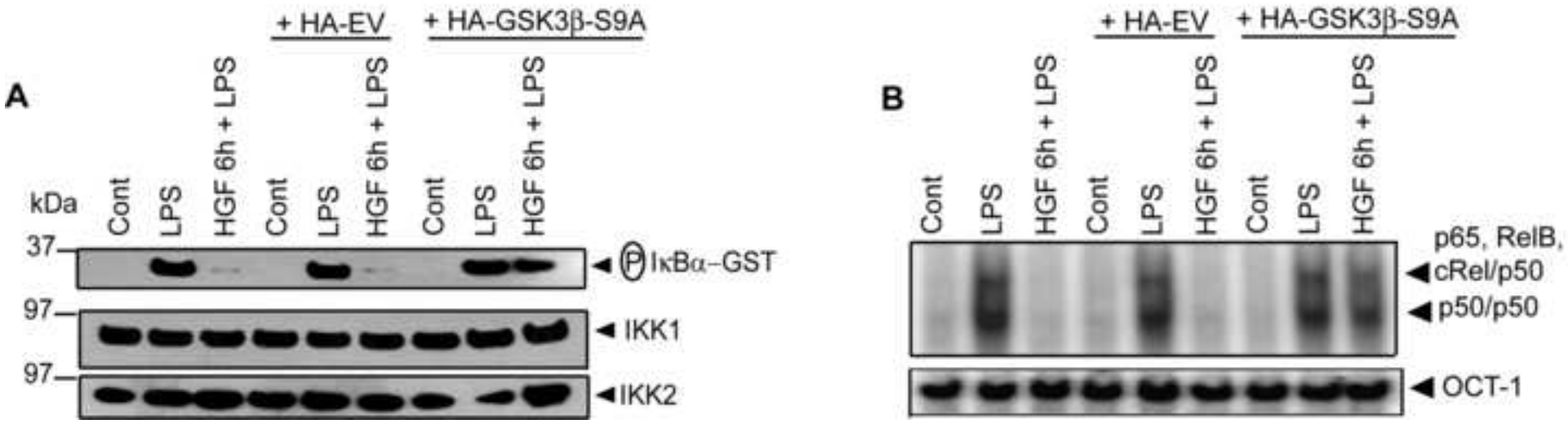

Figure-8

Click here to download high resolution image

FIGURE-8

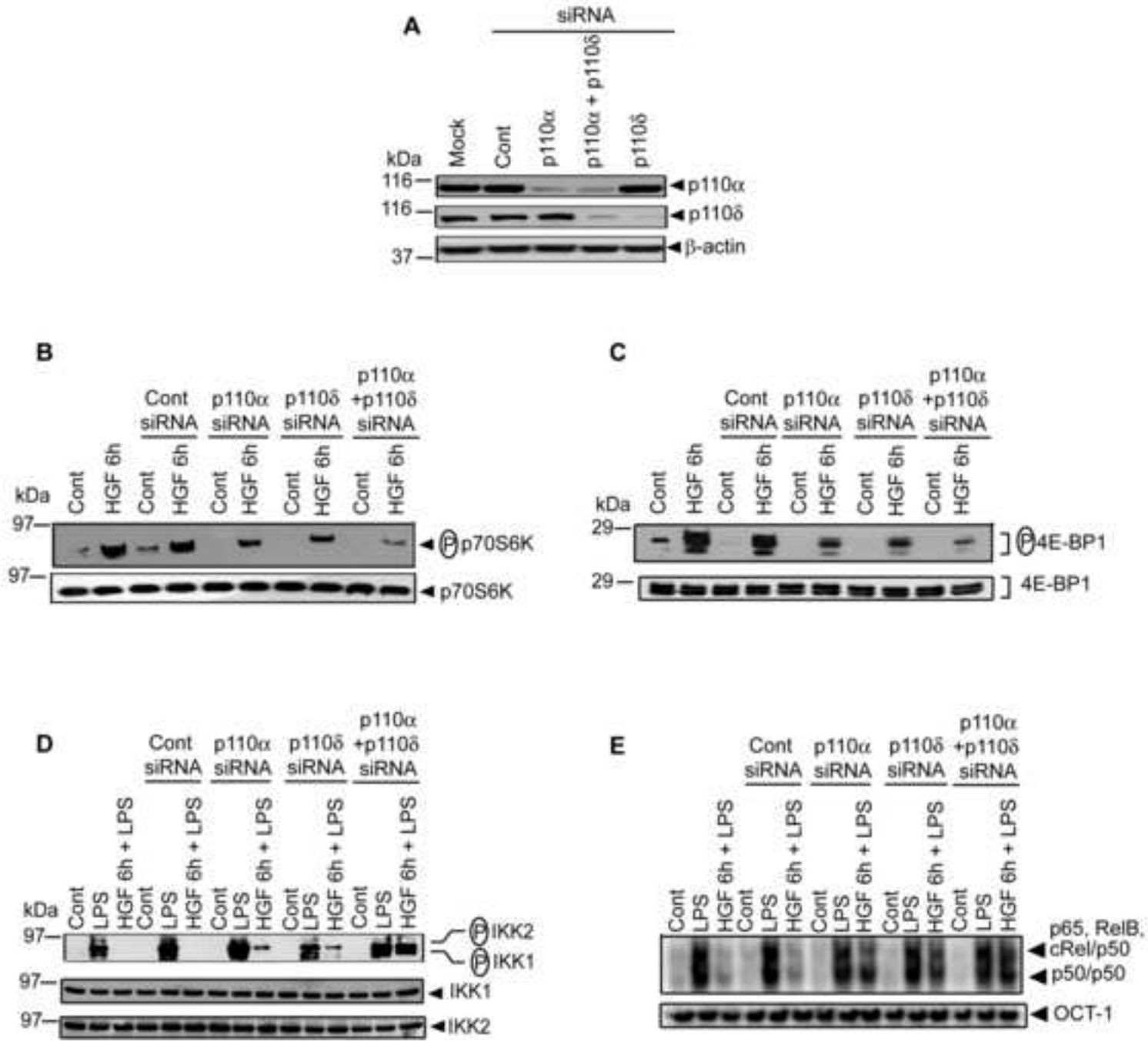

Figure-9

Click here to download high resolution image

FIGURE-9

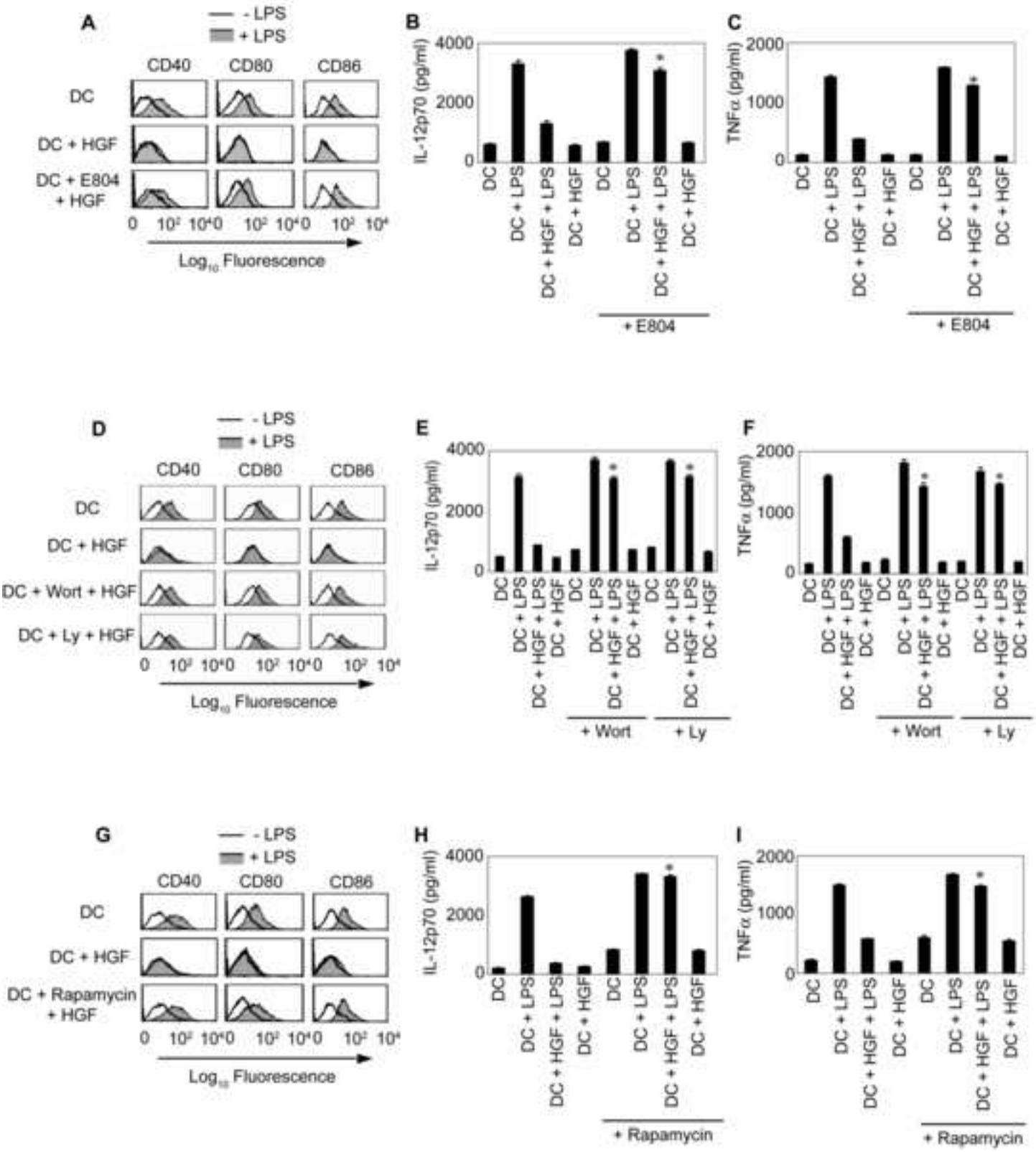

Supplemental Figure-1

Click here to download high resolution image

SUPPLEMENTAL FIGURE-1

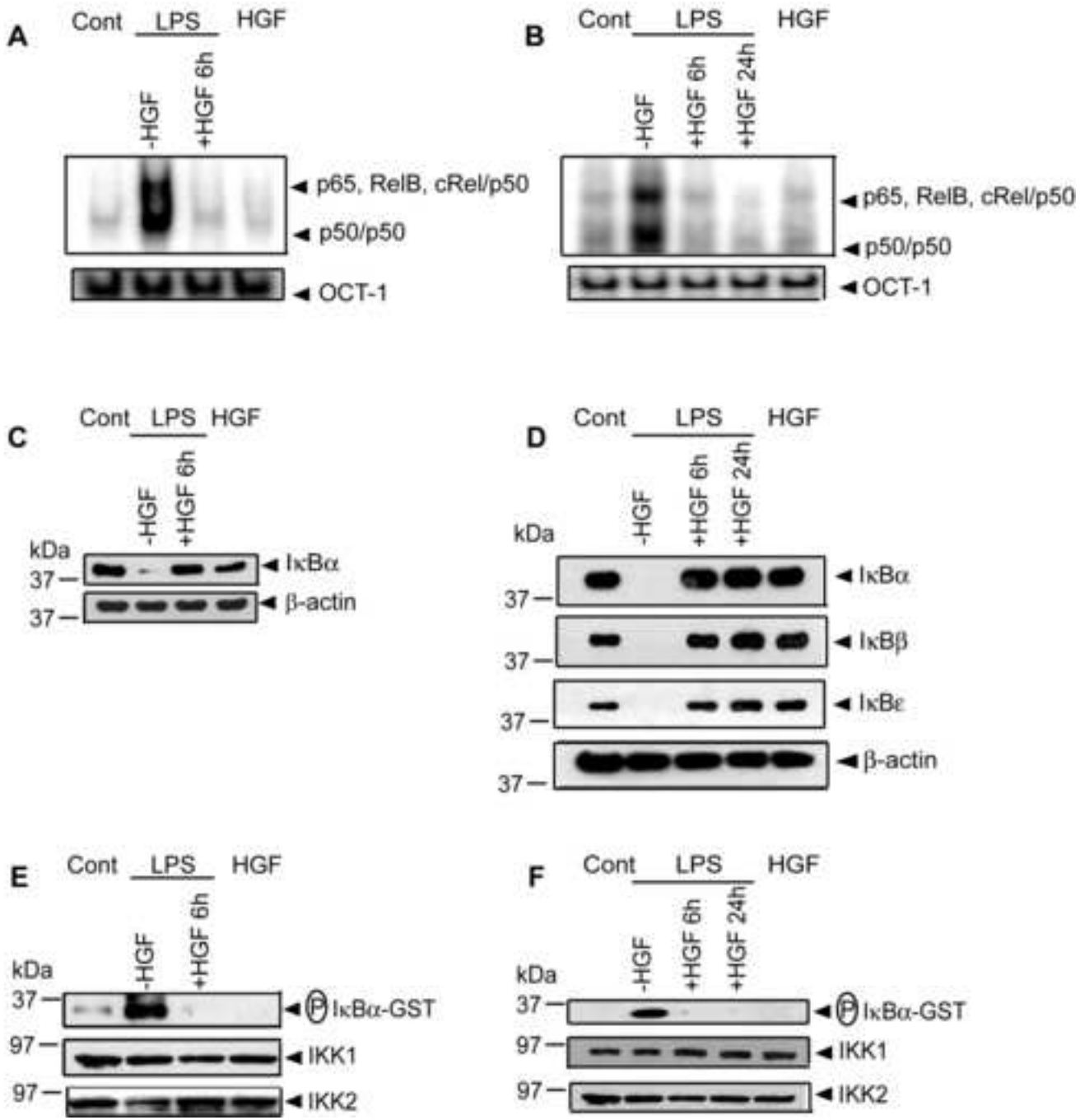

Supplemental Figure-2
Click here to download high resolution image

SUPPLEMENTAL FIGURE-2

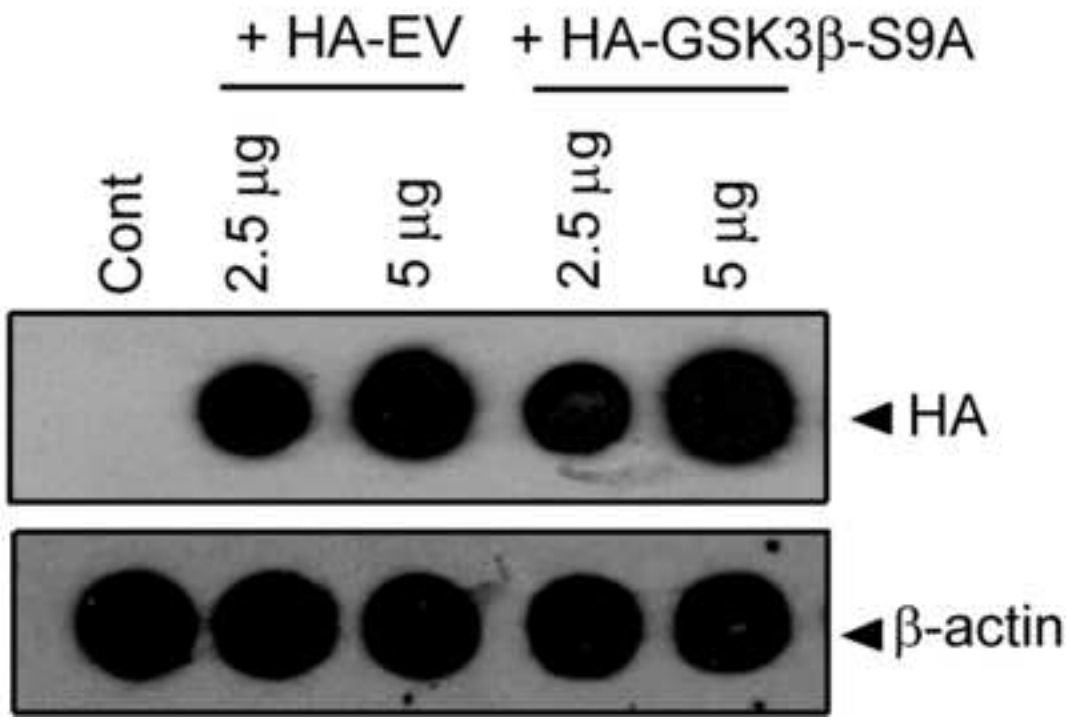

Supplemental Figure-3
Click here to download high resolution image

SUPPLEMENTAL FIGURE-3

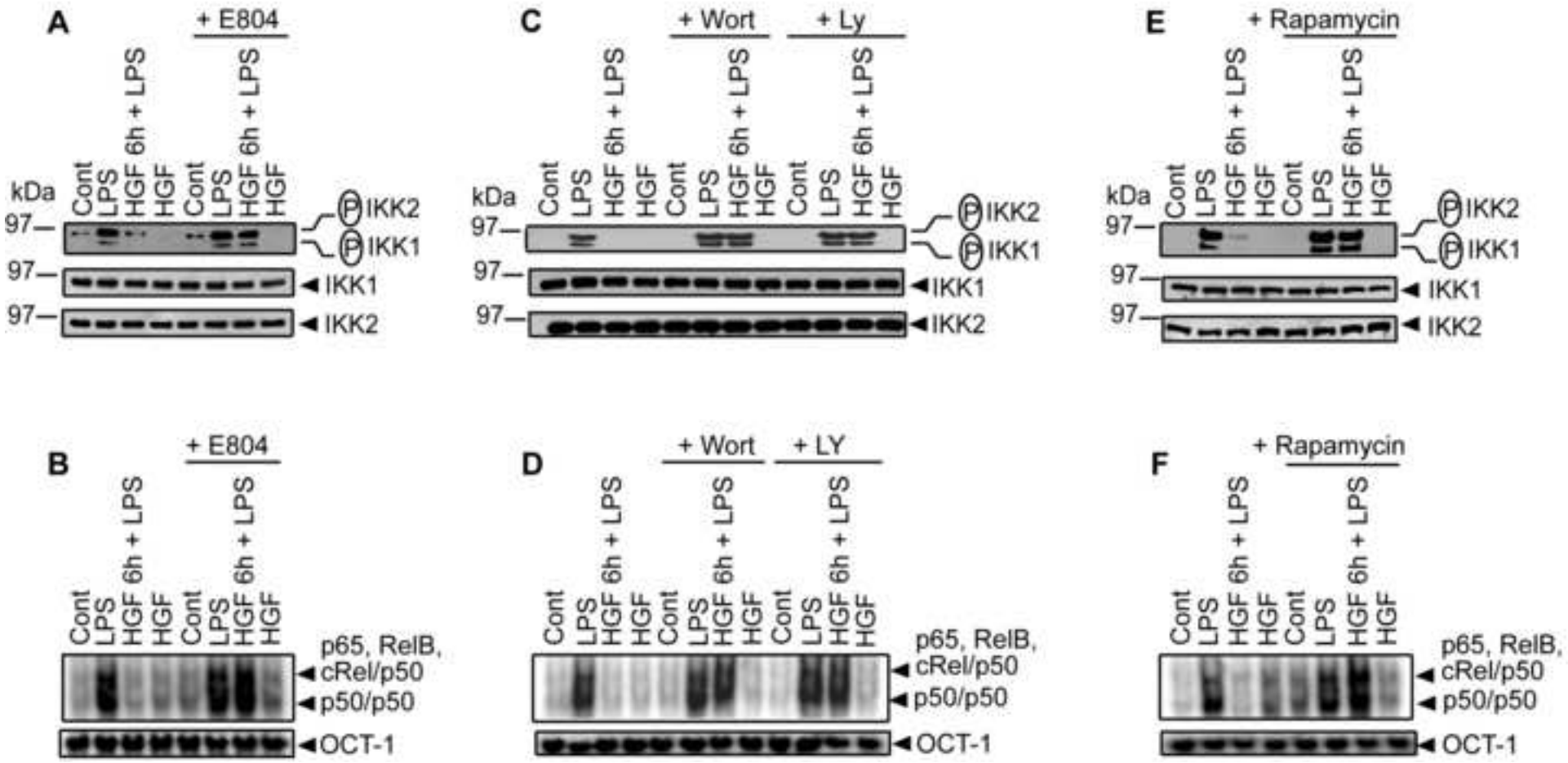

Supplemental Figure-4
Click here to download high resolution image

SUPPLEMENTAL FIGURE-4

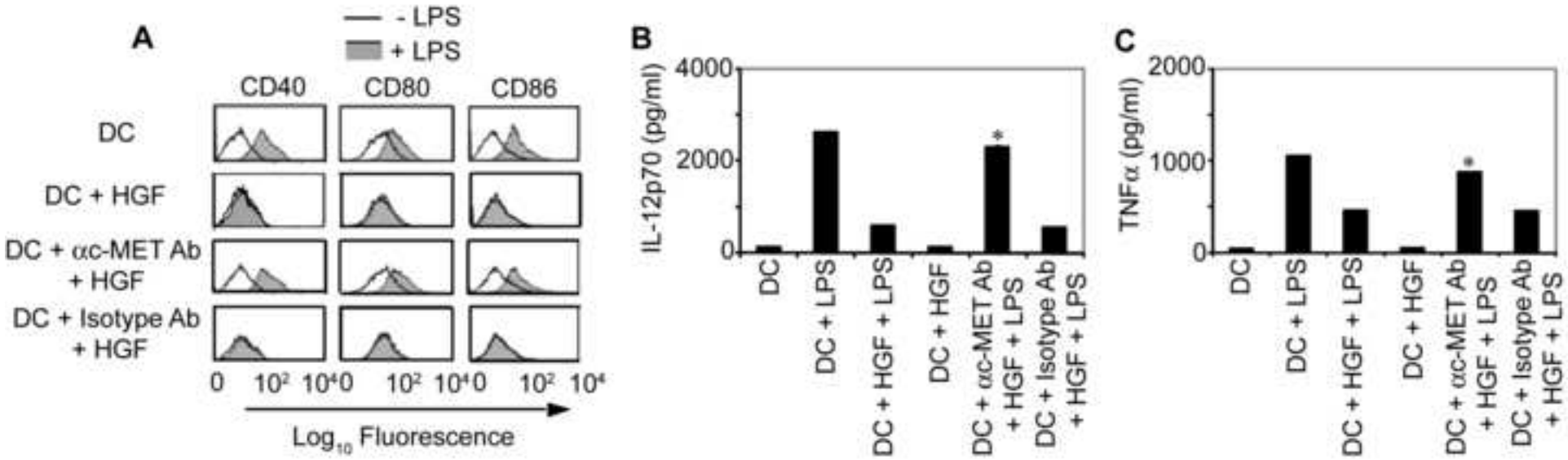

Supplemental Figure-5

Click here to download high resolution image

SUPPLEMENTAL FIGURE-5

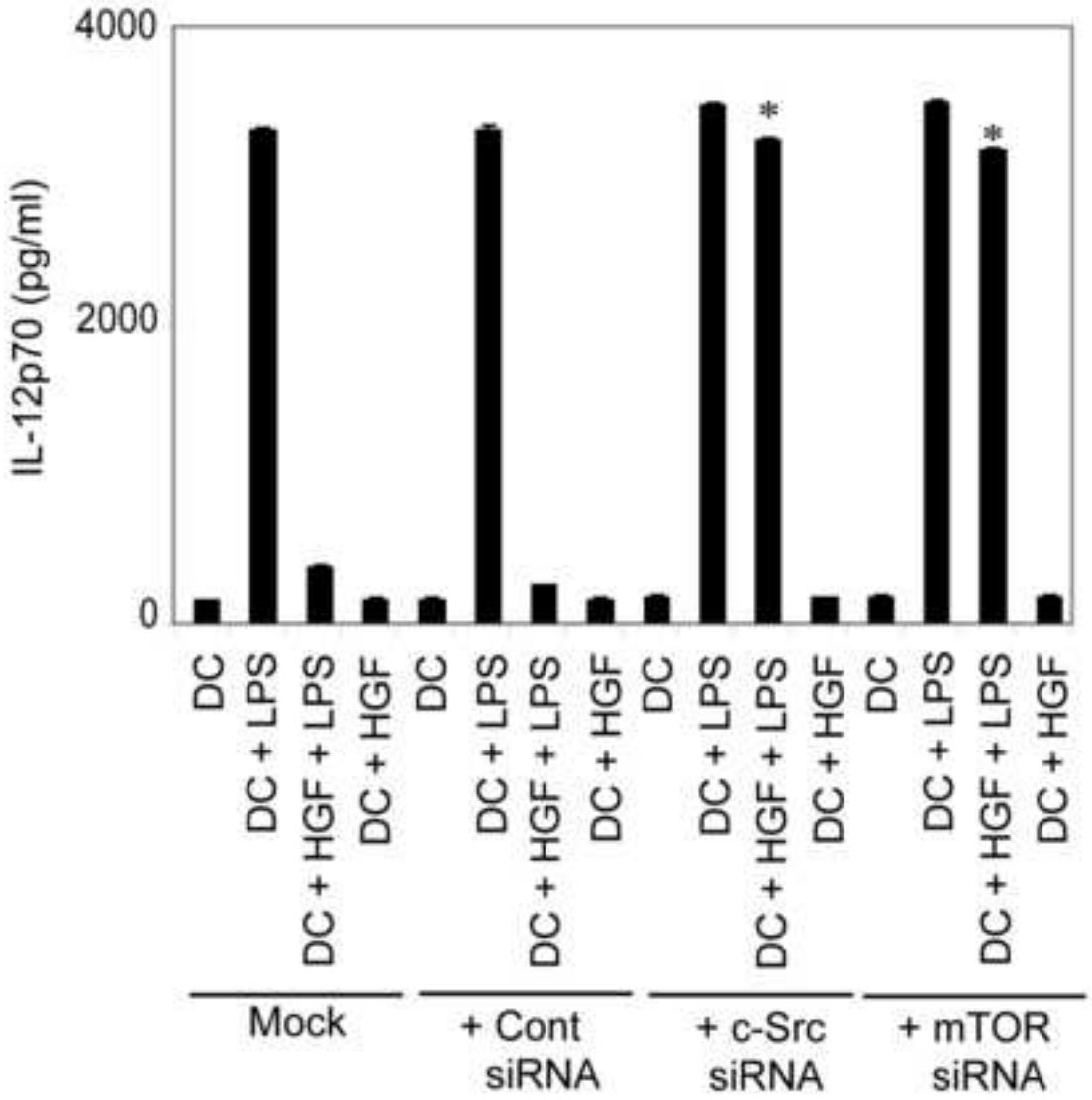

Supplemental Figure-6
Click here to download high resolution image

SUPPLEMENTAL FIGURE-6

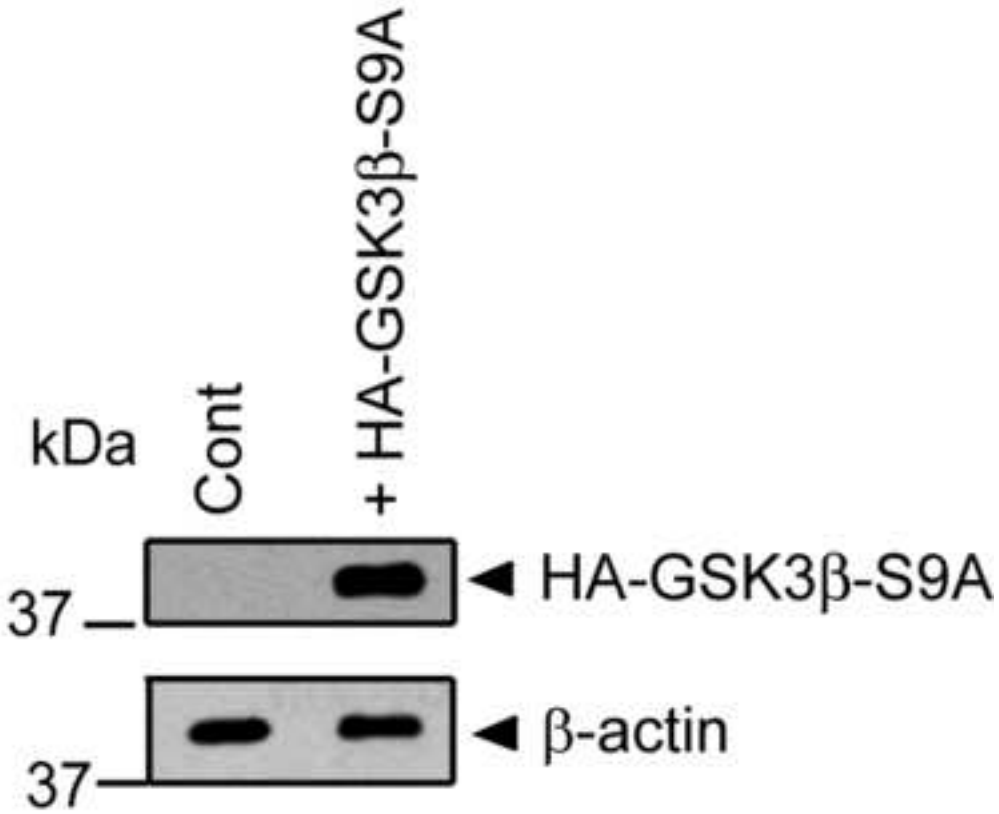

Supplementary Files

Click here to download Supplementary Files: SUPPLEMENTAL FIGURE LEGENDS.doc